

The background of the entire page is a photograph of a night sky. A vibrant green aurora borealis (northern lights) is visible as a horizontal band of light across the middle of the frame. Above the aurora, the sky is dark and filled with numerous small, bright stars. Below the aurora, the landscape is dark and silhouetted, showing rolling hills or mountains. The overall color palette is dominated by dark blues, blacks, and the bright green of the aurora.

An Overview on Orbit Determination Techniques for TLE Generation

Paul Schattenberg

An Overview on Orbit Determination Techniques for TLE Generation

PAUL SCHATTENBERG

**A LITERATURE STUDY
FOR THE
MASTERS OF SCIENCE DEGREE IN
AEROSPACE ENGINEERING
TECHNICAL UNIVERSITY OF DELFT**

DELFT, NETHERLANDS

Copyright © 2017 by Paul Schattenberg
Cover Illustration Copyright © 2016 by Paul Schattenberg

All rights reserved. This work or any portion thereof may not be reproduced or used in any manner whatsoever without the express written permission of the author except for the use of brief quotations in a review or scholarly journal.

First Printing: 2016

Paul Schattenberg
5305 Wolf Run
Austin, Texas 78749-1276

2 3 4 5 6 7 8 9 10

"I play to learn."
Charlotte Elvstrøm

Table of Contents

CHAPTER 1	INTRODUCTION.....	1
CHAPTER 2	A BRIEF HISTORY AND OVERVIEW OF TLES	3
	2.1 BACKGROUND INFORMATION	3
	2.2 AN OVERVIEW OF A TWO-LINE ELEMENT	5
	2.3 TLE LINE 1.....	7
	2.4 TLE LINE 2.....	8
	2.5 CONCLUSION	11
CHAPTER 3	ORBIT PROPAGATION TECHNIQUES	13
	3.1 BACKGROUND INFORMATION	13
	3.2 NUMERICAL INTEGRATION	16
	3.3 CLOSED FORM SOLUTIONS	18
	3.4 CONCLUSION	25
CHAPTER 4	MODERN ORBIT DETERMINATION TECHNIQUES	29
	4.1 BACKGROUND INFORMATION	29
	4.2 THE ORBIT DETERMINATION PROBLEM.....	32
	4.3 THE ORBIT DETERMINATION PROCESS.....	32
	4.4 THE DIFFERENTIAL CORRECTION PROCESS	42
	4.5 CONCLUSION	45
CHAPTER 5	CONCLUSION	47
APPENDIX A.	LIST OF VARIABLES	53
APPENDIX B.	LIST OF ACRONYMS	54
APPENDIX C.	TLE EXAMPLE.....	55
BIBLIOGRAPHY	57

Figures

FIGURE 2-1. FORTRAN 77 PUNCHCARD.....4

FIGURE 2-2. KEPLERIAN ORBIT ELEMENTS.5

FIGURE 3-1. THE EVOLUTION OF SATELLITE FORCE MODELS.....14

FIGURE 3-2. THE DIFFERENCES BETWEEN COMMON ORBIT PROPAGATORS.....18

FIGURE 3-3. VARIATIONS OF AN ORBITAL ELEMENT.....21

FIGURE 3-4. THE HONEYWELL 6080 COMPUTER.22

FIGURE 4-1. THE ORBIT DETERMINATION PROCESS.....33

FIGURE 4-2. GROUND STATION AND SATELLITE VECTORS.35

FIGURE 4-3. TRANSFORMATION OF COORDINATE SYSTEMS.....37

FIGURE 4-4. POSITIONING ESTIMATION-ERROR RESULTING FROM
MAGNETOMETERS AND SUN SENSOR DATA.42

FIGURE 5-1. ECLIPSE INTERVALS VS. ALTITUDE AND INCLINATION.50

FIGURE 5-2. WATERFALL GRAPH OF A SATELLITE PASS.52

Tables

TABLE 2-1. TLE LINE 1.....8

TABLE 2-2. TLE LINE 2.....10

TABLE 3-1. COMPARISON OF SPEED AND ACCURACY OF PROPAGATORS.....14

TABLE 3-2. COMPUTATIONAL SPEED OF PROPAGATORS IN 1988.25

TABLE 3-3. DIFFERENCES AMONG COMMON ORBITAL PROPAGATORS.....27

TABLE 4-1. OBSERVATIONAL DATA TYPES USED FOR ORBIT
DETERMINATION.30

TABLE 4-2. COMMON MEASUREMENT SETS FOR ORBIT DETERMINATION.31

TABLE 5-1. COMMON ERRORS IN DIFFERENT STAGES OF ORBIT
DETERMINATION.48

Chapter 1 Introduction

"To go places and do things that have never been done before - that's what living is all about."

- Michael Collins

In order to go places and do things that have never been done before with satellites and spacecraft, it is important to know where the spacecraft is, where it is going, and how it is going to get there. This report focuses on satellites orbiting Earth and brings together a collection of literature on the history and development of two-line elements, propagating orbits of satellites, and in tracking the satellites in order to update their Keplerian elements¹.

This report is divided into three main sections: 1) an overview in two-line elements, 2) the different types of orbit propagators, and 3) orbit determination. In Chapter 2, a brief history and overview of two-line elements is given. This section is important because two-line elements have a certain format that was established in the FORTRAN77 era that is still used today when disseminating the orbital parameters of satellites. These two-line elements not only contain the Keplerian orbital elements, but also contain important information such as drag terms and rates of change in the period of the satellite's orbit.

In Chapter 3, the different methods and techniques used for orbit propagation are explored. Over the years, many proposed solutions for propagating the position of satellites have been proposed. Today, there are two

¹ Also referred to as *TLEs*.

main methods of doing this: numerical integration and closed-form solutions. Both techniques provide very similar results, but the theory and methodology used, and computational time required to get to the results vary. Thus, it is important to explain the methodology and any simplifications made in determining the position and velocity of the satellite at any given point in time.

By taking two-line elements, not only can the location of the satellite as viewed from an observer be determined, but also important statistical information such as the distance to the satellite, how fast it is traveling relative to an observer, how long the satellite will appear overhead, and its current earth-centric latitude and longitude location can be calculated.² This information is valuable because as the motion of the satellite is propagated forward in time, errors increase. This reduces the ability to accurately determine the current location of the satellite and ultimately the positional estimates of the satellite. Therefore, there needs to be a way to refine the orbital estimations.

In Chapter 4, this refinement technique is discussed as well as modern orbit determination techniques used today. In order for this to be possible, multiple observations of the satellite need to be made. How these observations are made varies. Traditionally, RADARs and cameras that were used to detect airborne missiles during the Cold War provided sufficient results. However, these provided uncertainties in the along-track, cross-track, and altitude of the satellite that were relatively large. This required that the Keplerian elements of the satellites needed to be updated quite regularly. Today, techniques that are more sophisticated use some combination of RADAR, cameras, and lasers. Lasers drastically improve the altitude estimation for satellites, but unfortunately, errors in the along-track and cross-track positioning of the satellite remain. Nevertheless, this section brings together literature that details the processes used in the past and to-date in determining the orbit of the satellite.

Finally, Chapter 5 brings together all of the previous chapters, and poses the question: Where can changes be introduced to improve upon the orbital estimation of a satellite? Here within, a brief examination of the full block diagram of the technique used for orbit determination and the individual accuracies throughout parts of the system will be outlined.

So without further ado, let us get started!

² This is not fully discussed within this report. More information can be found in John A. Magliacane's source code for *PREDICT* (Magliacane, 2006).

Chapter 2 A Brief History and Overview of TLEs

"I suppose we shall soon travel by air-vessels; make air instead of sea voyages; and at length find our way to the Moon, in spite of the want of atmosphere."

- Lord Byron, 1822

2.1 Background Information

With the beginning of the space race during the 1950's, people needed to develop a method to track satellites in space. These methods needed to be capable of not only tracking satellites with high accuracy but also allow for the orbital elements of the spacecraft to be updated relatively fast. The first model was developed by Brouwer and Hori in 1959 (Vetter, 2007, p. 244). This model took into account a non-rotating spherical atmospheric model of the Earth. However, one particular person, Max Lane, discovered that the Brouwer-Hori's model had "no physical justification because the disturbing forces are intricately coupled" (Lane M. H., 1965, p. 2). Thus, Lane began building upon the Brouwer-Hori model and developed an enhanced mathematical satellite prediction model that incorporated a "non-rotating spherical power function model of the atmosphere" (Lane M. H., 1965, p. 1).

In August of 1969, Lane and Crawford published an article titled "An Improved Analytical Drag Theory for the Artificial Satellite Problem." This paper (an extension of Max Lane's original work) presented a numerical solution "for satellite orbits in a non-rotating atmosphere which takes into account the coupled

effects of atmospheric drag, and the second, third, and fourth zonal harmonics" (Lane & Crawford, 1969).

During the following decade, the North American Aerospace Defense Command (NORAD) developed an improved version of this 1969 Lane and Crawford model. For this model, NORAD developed two punch card formats that were used for storing the orbital elements of a satellite as well as other important information of interest. These are the *Internal* and *Transmission Format*. The *Internal Format* required the use of three punch cards (Figure 2-1) whereas the *Transmission Format* required only two.



Figure 2-1. FORTRAN 77 Punchcard.

In both formats, the first two punch cards contained all the necessary orbital elements of the satellite for orbit propagation. The third punch card of the *Internal Format* contained the other important information of interest, namely the country of origin, orbit type, operational frequency, and a general comments field. Since the third punch card of the *Internal Format* was of no use to orbit determination and the *Transmission Format* contained all the necessary information to compute the orbit of a satellite, the term "Two-Line Elements," commonly referred to as TLEs, later resulted from the use of the two cards of the *Transmission Format* for orbit propagation.

While punch cards might not be widely used today, the term has stuck and the *Transmission Format* is still used as the *de facto* standard when it comes to disseminating the required orbital elements needed to predict the location of satellites in space.

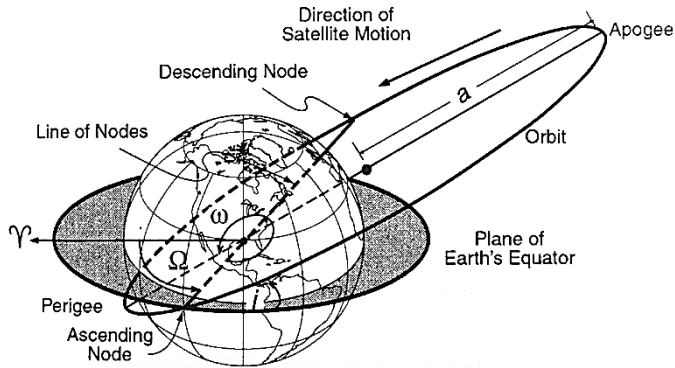


Figure 2-2. Keplerian Orbit Elements. Adapted from "Mission Geometry; Orbit and Constellation Design and Management" by J. R. Wertz, et al., 2001, p. 47. Copyright 2001 by Microcosm, Inc.

2.2 An Overview of a Two-Line Element

In the punch card era, each column meant something different. This carried over to modern times and the same rule applies to TLEs with each column (or sets of columns) containing very specific data. Furthermore, it is from this specific set of information, that a satellite's orbit can be computed. The symbols used within this report are all defined in Appendix A.

In order to propagate a satellite forward in time, Keplerian orbital elements are needed to describe an orbit (Wertz, et al., 2001, pp. 45-52). These are the satellites:

1. Semi-major axis, a ,
2. Eccentricity, e ,
3. Inclination, i ,
4. Right ascension of the ascending node, Ω ,
5. Argument of perigee, ω , and the
6. True anomaly, v , or mean anomaly, M .

Of these six Keplerian elements, the first two (a and e) set the shape and size of the orbit. The next two elements (i and Ω) define the plane of the orbit. The argument of perigee defines the rotation of the semi-major axis with respect to the Earth's equatorial plane. Finally, the true or mean anomaly describes the position of the satellite in its orbit at a specified time. With these six classical Keplerian elements, the satellite's position can be calculated at a specific time in the past, present and/or future. Figure 2-2 illustrates these Keplerian elements.

Unfortunately, Keplerian elements alone are not accurate enough in calculating the precise position and velocity of the spacecraft at a given time since other atmospheric and gravitational effects need to be taken into account. However, they are usually considered accurate enough to estimate the characteristics of the mission (Wertz, et al., 2001, p. 52). Therefore, if more precise calculations are needed, additional oscillatory perturbations need to be accounted for in the orbit propagation model. These additional perturbations are described further in Chapter 3 when looking at orbit propagation models. Nevertheless, they can be grouped into four distinct categories (Wertz, et al., 2001, p. 62):

1. Non-gravitational interactions,
2. Third-body interactions,
3. Non-spherical mass distributions, and
4. Relativistic effects³.

The following lines are an example of a Two-Line Element set⁴ for the International Space Station as generated on 8 October 2016 at 01:05:00 UTC⁵:

```
123456789 123456789 123456789 123456789 123456789 123456789 123456789
1 25544U 98067A 16280.54513569 .00016717 00000-0 10270-3 0 9035
2 25544 51.6411 222.5831 0007033 41.1186 319.0496 15.54057571 22306
```

The first column of both cards represents the line number (1 & 2); columns three through seven are the United States Space Command assigned satellite number (25544), and the last column (Column 69) is the checksum of the TLE⁶. For now, the focus is on the first line, starting with column eight. Column 8 represents the classification of the satellite. This single character can be either a U for *unclassified* satellites, a C for *classified* satellites, or an S for satellites classified as being *secret*.

³ Relativistic effects are generally ignored, as their perturbation effects are small.

Example: Mercury experiences a relativistic perturbation in its orbit of 0.012° per 100 years (Wertz, et al., 2001, p. 62).

⁴ The first row is only for counting column numbers and is not a part of the TLE.

⁵ Universal Coordinated Time. Also known as Greenwich Mean Time.

⁶ More information on how the checksum is calculated be found in (Vallado, Crawford, Hujsak, & Kelso, 2006, pp. 4-5) and (Magliacane, 2006).

2.3 TLE Line 1

Columns 10 through 17 represent the international designator (98067A) with the first two numbers representing the last two digits of the launch year of the satellite (i.e. 1998), and the three numbers that follow represent the launch number of that year (067). The remaining digits or numbers identify the piece number of the launch. These are the only items that remain constant for TLEs with the rest of the data subject to change.

The next block of data on line one is the time at which the observation was made (16280.54513569). This is commonly referred to as the *epoch time*. The first two numbers of the epoch time signify the last two digits of the year for which this particular observation was made (2016) with all numbers less than 50 being representative of the years after 2000 (Vallado, Crawford, Hujsak, & Kelso, 2006, p. 56). The remaining numbers (280.54513569) are the decimal count of how many days have passed since the beginning of that particular year.

The next two sets of numbers represent $\dot{n}_0/2$ (column 34 to 43) and $\ddot{n}_0/6$ (column 45 to 52). The first position in each of these numbers (column 34 and 45) are signing columns. If the number that follows is negative, these two columns have a "minus sign." The number that results ($\ddot{n}_0/6$) from column 46 to 50 is assumed to have a decimal point before the number. In other words, the number that comes from column 46 through 50 is always multiplied by 0.00001. Similarly for $\dot{n}_0/6$, column 51 is a signing symbol for the exponent in column 52. For example, $-12345-6$ would be interpreted as $-0.12345E-6$.

Column 51 to 61 is the B^* term. This term is "used to estimate the drag force felt by the object in orbit" (Miura, 2009).

Column 63 is more of historical value and results from the punch card era. Nowadays, this spot is set to zero (AIG, 2016). However, from a historical perspective, it contained a single number varying from one to/and including five and allowed the user to select the ephemeris type for orbit propagation (Hoots & Roehrich, 1980, pp. 70-72,76) (Vallado, Crawford, Hujsak, & Kelso, 2006, p. 4). Should the number in this location ever be a number other than zero, then it is recommended to use the corresponding propagator (AIG, 2016).⁷

The next set of numbers on line one (column 65 through 68) contains the element set number that increases by one every time a new TLE set is generated for that specific satellite.

⁷ 1 = SGP, 2 = SGP4, 3 = SDP4, 4 = SGP8, 5 = SDP8 (Hoots & Roehrich, 1980, p. 76)

A summary of TLE Line 1 is presented below in Table 2-1 for the aforementioned explanation.

123456789 123456789 123456789 123456789 123456789 123456789 123456789
1 25544U 98067A 16280.54513569 .00016717 00000-0 10270-3 0 9035

Table 2-1. TLE Line 1.

COLUMN	CONTENT	EXAMPLE
1	TLE Line Number	1
3-7	Satellite Number	25544
8	Satellite Classification	U - Unclassified
10-17	International Designator	98067A
19-32	Epoch Time	16280.54513569
34-43	$\dot{n}_0/2$	0.00016717
45-52	$\dot{n}_0/6$	00000-0
54-61	B*	0.10270E-3
63	Ephemeris Type (Unused)	0
65-68	Element Set Number	903
69	Modulus 10 Checksum	5

2.4 TLE Line 2

Columns one through seven are the same as those found in TLE Line 1., where the first column represents the line number of the Two-Line Element and columns three through seven are the United States Space Command assigned satellite number (25544).

The first two sets of numbers located in columns 9 through 16, and columns 18 through 25, define the orientation of the orbit plane. Respectively, these are the inclination, i_0 , and right ascension of the ascending node, Ω_0 .

On the TLE, the inclination, i_0 , is expressed in degrees. For satellites orbiting around Earth, the inclination is defined as the angle between the orbital plane of the satellite and the Earth's *equatorial plane* (Wertz, et al., 2001, p. 47). Angles are always positive and taken on the ascending node⁸. Thus, the inclination will always be between 0 and 180 degrees. A satellite is said to be in a prograde orbit if the inclination is between 0 and 90 degrees. This means that the satellite

⁸ The location of the ascending node is the location where the satellite crosses the equator from the southern to northern hemisphere.

travels counter-clockwise (or orbits in the same direction as the rotation of the Earth). For a satellite with an inclination above 90 degrees, the satellite is said to be in a retrograde orbit (or against the rotation of the Earth). For this particular TLE, the satellite's orbital plane is rotated 51.6411 degrees from the equator in a prograde orbit.

Another interesting property of the inclination is that this number also defines the highest or lowest latitude that the satellite can be seen directly overhead. Thus, someone living at a latitude higher (or lower) than 51.6411 degrees north (or south) will either never see the satellite⁹ or it will never appear directly overhead.

Following the inclination is the right ascension of the ascending node, Ω . This variable is also expressed in degrees (222.5831 degrees). The right ascension of the ascending node (RAAN) is the angle measured eastward between the location of the First Point of Ares¹⁰ and the intersecting point of the ascending node of the orbital plane with Earth's equatorial plane.

Next, is the eccentricity, e_0 , of the satellite (column 27 through 33). This is the number that defines the shape of the orbit. A decimal point is assumed to exist before the number. Therefore, the number 0007033 in this eccentricity example is actually 0.0007033. A satellite with an eccentricity of zero is in a circular orbit around Earth and values between zero and one form an elliptical orbit. Values larger than or equal to one represent a parabolic or hyperbolic escape orbit.

Fortunately, only one orbital element is needed to calculate the rotation of the orbit plane of the satellite with respect to the Earth's equatorial plane. This is called the *Argument of Perigee*. The Argument of Perigee is the angle between the line joining the center of the Earth, the right ascension of the ascending node, and the location of the satellite on the closest approach (expressed in degrees) as

⁹ With the maximum or minimum latitude that the satellite can physically be seen being defined by the slant range of the satellite plus the inclination.

¹⁰ The First Point of Ares is the zero-point for the right ascension. This point is defined as the longitudinal location of the ascending node of Earth's orbit with respect to the Sun on the first day of spring. One of the drawbacks to using this location is the fact that Earth experiences a 26,000-year precession. Thus, all coordinate systems usually have a date associated with them. Most satellites use "true-of-date coordinates" where the vernal equinox is calculated at the time specified on the Two-Line Element. However, some will use the coordinate system corresponding to the year 2000. Unfortunately, this makes it difficult to verify orbit computations since there is a small difference in coordinate system specifications.

Table 2-2. TLE Line 2

123456789 123456789 123456789 123456789 123456789 123456789 123456789
2 25544 51.6411 222.5831 0007033 41.1186 319.0496 15.54057571 22306

COLUMN	CONTENT	EXAMPLE
1	TLE Line Number	2
3-7	Satellite Number	25544
9-16	Inclination	51.6411 [deg]
18-25	RAAN	222.5831 [deg]
27-33	Eccentricity	0.0007033 [-]
35-42	Argument of Perigee	41.1186 [deg]
44-51	Mean Anomaly	319.0496 [deg]
53-63	Mean Motion	15.54057571 [Orbits/day]
64-68	Number of Orbits	2230
69	Modulus 10 Checksum	6

measured counter-clockwise. This angle is represented in column 35 to 42 (ex. 041.1186 degrees). A satellite with an Argument of Perigee of zero degrees means that the perigee, or its closest approach, happens at the right ascension of the ascending node (where the satellite crosses from the southern to northern hemisphere). Similarly, an angle of 270 degrees would suggest that the satellite's closest approach occurs at the southern-most point in the satellites orbit.

One of the Keplerian Elements that is difficult to calculate is the *True Anomaly*, v . This parameter defines where the satellite currently is located in its orbit. It is the angle between the center of gravity of the satellite and the perigee of the orbit (as defined by the *Argument of Perigee*). Since this particular term is difficult to calculate, modern techniques employ the use of an additional variable, the *Mean Anomaly* (Column 44-51: 319.0496 degrees). This number is defined as the amount of time that has passed since perigee passage, divided by the orbital period. More about this variable is presented in Chapter 3.

The last of the orbital elements that are presented in the Two-Line element is the Mean Motion, n_0 (column 53-63). This number is the number of revolutions the satellite can make around Earth in a day (assuming a constant-speed circular orbit). Thus, the satellite in this particular example can complete 15.54057571 orbits per day. It should be noted that this number is not an average of the number of revolutions the satellite makes in a day, but is instead an instantaneous calculation using the gravitational parameter, μ , and the satellites semi-major axis, a .

The last number found in column 64 to 68 is of no particular use to orbit propagation. Nevertheless, it represents the number of orbits that have occurred between the time the satellite was launched and that of the epoch time found in line 1. In this example, that number is 2230.

A summary of TLE Line 2 is presented in Table 2-2 for the aforementioned explanation.

2.5 Conclusion

Two-line elements have historical roots dating back to the 1960s. The *Transmission Format* still serves as the *de facto* standard format used today to distribute and update information about a satellite's orbit.¹¹ This format distributes the bare minimum information needed to calculate the location of a satellite and propagate its orbit accurately. Six elements are needed in order to define an orbit. Five of them are given directly on the two-line elements¹², and one of them, the semi-major axis, a , needs to be calculated from the mean motion¹³ in order to recover all six Keplerian orbital elements. These six Keplerian elements are sufficient to calculate the position and velocity of the spacecraft at the time specified in the element set; however, they alone are not sufficient if the location of the satellite is to be calculated at another instant in time.

Because of this, since the late 1950s, orbital models have been developed, with each iteration introducing simplifications in orbital dynamics while becoming more sophisticated. Each model built upon previous work and introduced something new to the underlying equations in order to refine the accuracy of the models. In the next chapter, these propagation models are examined.

¹¹ Sections 2.3 and 2.4 explained these lines in detail. A summary of two-line elements can be found in Appendix C.

¹² These are the inclination, RAAN, eccentricity, argument of perigee, and the mean anomaly of the satellite.

¹³ See equation for a in (Hoots & Roehrich, 1980, p. 3) and in subsequent sections within the same report.

Chapter 3 Orbit Propagation Techniques

"Keep looking up... that's the secret of life..."

- Charles M. Schultz

3.1 Background Information

Since the 1950s, there have been many proposed techniques and methods for tracking satellites. The history and development of orbit propagation models is shown in Figure 3-1. Of these, the Simplified General Perturbation Theory Nr.4 (SGP4) has become the *de facto* standard for tracking satellites. This standard resulted from a report published in 1978 by NORAD. In the report, it outlined the information processing capabilities of the organization. Furthermore, it stated that all space-borne objects were originally to "be tracked with AFGP4 accuracy; however, due to limited capabilities of [their computers], DP-4 and SGP-4 will be used" instead (Staats, 1978, p. 17). Thus, NORAD ultimately sacrificed accuracy to computational speed to track the *4,000 plus*¹⁴ space-borne objects (Table 3-1).

¹⁴ This is at the time of NORAD's publication in 1978.

Table 3-1. Comparison of Speed and Accuracy of Propagators. Adapted from *NORAD's Information Processing Improvement Program* (p. 17), by E. B. Staats, 1978, Copyright 1978 by NORAD.

PROGRAM SYMBOL	ACCURACY	SPEED
DP-4	Low	High
SGP-4	Low	High
IGP-4	Medium	Medium
AFGP-4	High	Low
SPECIAL PERTURBATIONS	Very High	Very Low

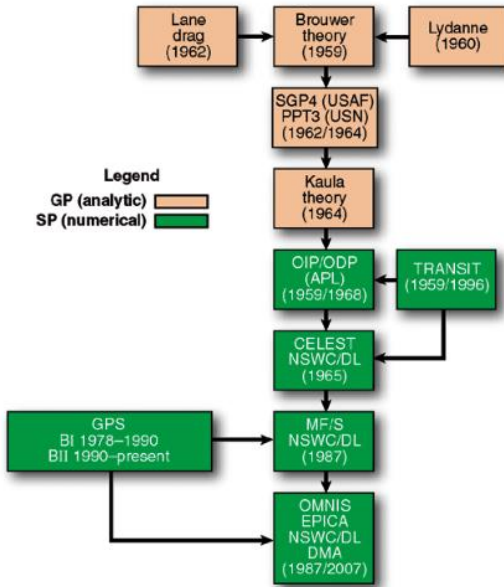


Figure 3-1. The Evolution of Satellite Force Models. Adapted from "Fifty Year of Orbit Determination" by J. R. Vetter, 2007, *Johns Hopkins APL Technical Digest*, 27, p. 244. Copyright 2007 by J. R. Vetter.

In order to understand fully how to implement a satellite prediction program, it is appropriate to examine an implementation of satellite tracking and orbit propagation source code. By analyzing source code from satellite tracking software, one can determine how to implement a satellite prediction program and

cross-reference the algorithms presented in the source code with the algorithms found in public domain material¹⁵ to verify the algorithms.

Tracking a satellite from a location on the ground can be broken down into the following sections and steps (Magliacane, 2006) (Schattenberg, 2015):

Satellite:

1. Extract orbital elements from two-line elements (TLE).
2. Obtain the current date in Julian days.
3. Determine the amount of time that has passed between the current date and the time since the TLE was generated (in minutes).
4. Using the data provided by the TLE and one of the satellite propagators (discussed in section 3.2 and 3.3), propagate the satellite's location forward in time to a user-selected date to extract the position and velocity vectors of the satellites location at that user-specified time.

Ground Station:

1. Obtain the current latitude, longitude, and altitude of the ground station location,
2. Propagate the observer's location forward in time to that of the time of interest.
3. Convert this location into the observer's position and velocity vectors in the same reference frame as the tracked satellite.

Ground Station and Satellite:

1. Determine if the acquisition of signal is possible, if the satellite has decayed, or if the satellite is geostationary,
2. Calculate observation angles: azimuth, elevation, range, and range rate,
3. Calculate the satellite's sub-satellite point: latitude, longitude, and altitude,
4. Calculate the satellite's right ascension and declination, and
5. Calculate other miscellaneous statistics; such as, footprint width, Doppler shift, eclipse depth, and orbital phase.

¹⁵ (Magliacane, 2006), (Hoots & Roehrich, 1980), and (Vallado, Crawford, Hujsak, & Kelso, 2006)

It should be worth noting that the algorithms used in the program *Predict*¹⁶, were taken primarily from the documentation that can be found on Dr. Kelso's web site, CelesTrak¹⁷. On his website, Dr. Kelso outlines the algorithms and methods needed in order to perform orbital propagation, orbit determination, orbital coordinate system transformation, and satellite pass predictions.

This chapter focuses on the "two primary computational methods of implementing an orbital model" used to propagate the satellite's location forward in time to a user-selected date from a TLE (Kelso, 2014).¹⁸ All of the propagators express and/or account for the acceleration-effects experienced by the satellite in a different manner. How these effects are accounted for is briefly explained in sections 3.2 and 3.3.

3.2 Numerical Integration

The slowest of the methods, numerical integration (*Special Perturbations*¹⁹ in Table 3-1), provides the most accurate estimate for orbit propagation. This method is particularly useful in determining how much of a force is acting upon a satellite at any given time. However, this method is slow as the position and velocity of the satellite must be calculated for each time step between the initial location and the time of interest (Kelso, 2014).

Numerical integration works on the principal of solving equation 3-1,

$$\ddot{\vec{r}} = -\frac{GM}{r^3}\vec{r} + f_G + f_{NG} \quad 3-1$$

where the term f_G and f_{NG} contain the sum of the gravitational and non-gravitational accelerations acting on the satellite, respectively²⁰.

¹⁶ <http://www.qsl.net/kd2bd/predict.html>

¹⁷ <https://celestrak.com/columns/>

¹⁸ via numerical or analytical (closed-form) calculations

¹⁹ The most common method is Cowell's Method. In this method, accelerations are integrated to determine the velocity and position of the spacecraft. (Berget, et al., 1992, p. 142)

²⁰ This is explained in more detail in section 4.2.

Numerical integration works as follows:

1. each individual force that is acting upon the satellite (right-hand side of equation 3-1) is evaluated,
2. The resulting acceleration is then used to determine the new position and velocity vector of the satellite for a very small time-step,
3. The satellite is then propagated the new location using the information from step 2, and the process repeats.

However, this method is by no means a trivial task. Taking into account and evaluating all the forces acting upon the satellite accurately is not an easy task, as all these forces vary with time, weather, and some are semi-unpredictable²¹ (Kelso, 2014). These forces include, but are not limited to:

1. a non-uniform mass and gravitational distribution of Earth (Wertz, et al., 2001, pp. 64-67),
2. gravitational accelerations a satellite will experience from the sun, planets, and moons,²²
3. solar radiation pressure²³, and
4. atmospheric drag²⁴.

Thus, due to the complex nature of this problem, limited computing power, and with having to monitor thousands of satellites (all for very small time-steps), numerical integration for keeping track of every satellite by NORAD was out of the question. Therefore, NORAD went with a faster, analytical approach for monitoring satellites.

With computers being much more powerful today, satellites can be tracked numerically a lot faster than before; however, Table 3-1 still remains. Nevertheless, this allows for high precision and accurate orbital simulations to be run. The main pitfall of numerical integration is computation time, as one must compute the location of the satellite at all time steps between the initial time and

²¹ i.e. solar cycles, CMEs, and solar flares.

²² Causes a periodic external torque in the satellite, which causes the angular momentum vector to rotate and affects all orbital elements (Wertz, et al., 2001, p. 67).

²³ Causes periodic variations in all orbital elements and is the strongest for low-mass/high area cross-section satellites (Wertz, et al., 2001, p. 67).

²⁴ Highly variable and impossible to predict. A major source of error. Depends on altitude and changes based upon solar activity (Wertz, et al., 2001, pp. 68-74).

the time of interest. Although less accurate but faster, this is what makes a closed-form solution attractive for orbit propagation and prediction models.

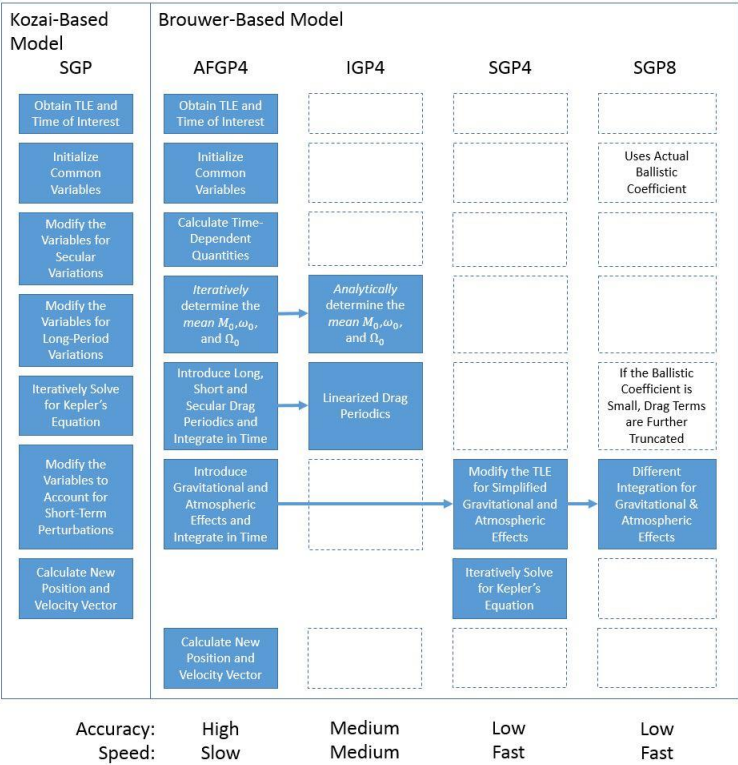


Figure 3-2. The Differences Between Common Orbit Propagators. Note. This graphic outlines the main differences between the two types of orbit propagation models: Kozai- and Brouwer-based theory. The arrows denote where modifications to the AFGP4 theory were made. The outlined boxes denote that nothing has changed between one model and the next, and the outlined boxes with text represent slight exceptions in the methodology.

3.3 Closed Form Solutions

In the late 1950's, two base-theories were being developed for orbit propagation: the Kozai and Brouwer theory. In this section, the main analytical drag theories that have been developed for orbit propagation will be examined,

specifically, the *General Perturbation*²⁵ theory sets. Here within, different closed-form analytical approaches are presented chronologically starting with the earliest used theory. Except for the perturbation theory presented in the section 3.3.1 and 3.3.2, all analytical drag theories are simplified versions the Air Force General Perturbation Theory Nr. 4 (AFGP4) (Lane & Hoots, 1979). A summary of these two models and the Brouwer-based theory differs are found in Figure 3-2.

The derivation and presentations of the following models can be found in their respective sources; however, each section, in order of development, will present a general outline on the orbital quantities that are calculated in each respective section.

3.3.1 Simplified General Perturbation Theory

The first model, Simplified General Perturbation Theory (SGP), is based upon the work of Kozai (Kozai, 1959) and Brouwer (Brouwer, 1964), and was later refined and made available by Hilton and Kuhlman (Hoots & Roehrich, 1980, p. 1). It was used to track near-Earth satellites²⁶ and served as "the original satellite motion model" (Ostrom, 1993) for the Air Force Space Command until 1976 when SGP4 was developed.

The Simplified General Perturbation model is characterized by the perturbing accelerations due to the oblateness and unequal mass distribution of the Earth,²⁷ and a symmetrical atmospheric drag model (Ostrom, 1993). Furthermore, mean motion perturbations are taken to be linear in time and "the drag effect on eccentricity is modeled in such a way that [the] perigee height remains constant" (Hoots & Roehrich, 1980).

The Simplified General Perturbation theory can be broken down into the following steps:

1. Obtain the orbital elements from a TLE and determine the time of interest for propagating the satellite.
2. Initialize common variables.
3. Modify these variables to include secular and long-period time-dependent perturbations due to gravitational and atmospheric drag effects.
4. Iteratively solve Kepler's equation to a desired accuracy.

²⁵ "General perturbations analytically solve for some aspects of the motion of a satellite subject to perturbing forces" (Berget, et al., 1992, p. 142).

²⁶ Near-Earth satellites are satellites with an orbital period less than 225 minutes.

²⁷ This is the Brouwer Geopotential Model.

5. Calculate short-term oscillating quantities and add these to the perturbed elements from Step 3.
6. Calculate the position and velocity vectors at the new time of interest.

3.3.2 Air Force General Perturbation Theory Nr. 4

As previously mentioned, the Air Force General Perturbation Theory (AFGP4) serves as the parent theory for all the remaining orbital propagators. In other words, all analytical drag theories are *simplified* versions of this theory.

The Air Force General Perturbation Theory is based upon work of Brouwer, Lane, and Crawford.²⁸ Aside from special perturbation numerical integration techniques, this model provides *high* accuracy; however, the computational speed of it is relatively slow when compared to the IGP4 and SGP4 propagators (Table 3-1). This model "includes the effects caused by the first five zonal harmonics of the Earth" and "assumes a static, non-rotating, spherically symmetrical atmosphere" (Herriges, 1988, p. 46) (Lane & Hoots, 1979, p. 1).

An explanation of the algorithm along with the sources of how it was derived can be found in *General Perturbations Theories Derived from the 1965 Lane Drag Theory* (Lane & Hoots, 1979). Nevertheless, it is summarized below:

1. Obtain the orbital elements from a TLE and determine the time of interest for propagating the satellite.
2. Initialize common variables.
3. Calculate time-dependent quantities.
4. Iterate the propagated *mean* mean anomaly, *mean* argument of perigee, and the *mean* right ascension of the ascending node until convergence.
5. Calculate the drag periodics.
6. Using these drag periodics, calculate the periodic perturbed orbital elements.
7. Add the oscillating gravitational effects of the Earth to the orbital elements.
8. Calculate the position and velocity vectors at the new time of interest.

²⁸ (Brouwer, 1964), (Lane M. H., 1965) and (Lane & Crawford, 1969).

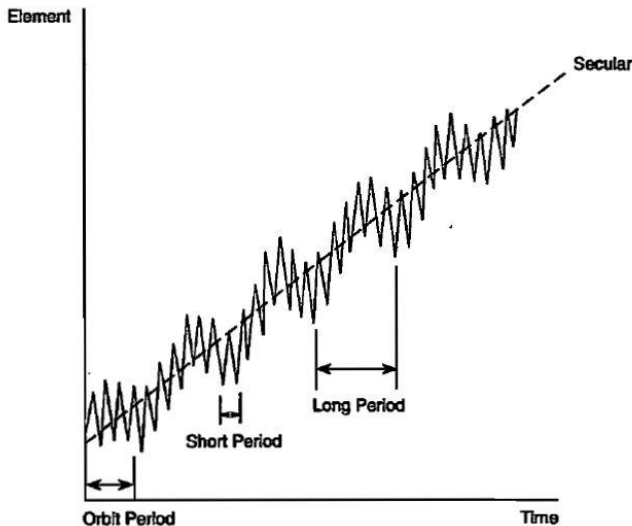


Figure 3-3. Variations of an Orbital Element. Note. "Secular variations represent linear variations in the elements, short-period variations have a period less than the orbital period, and long-period variations have a period longer than the orbital period" (Berget, et al., 1992, p. 141). Adapted from Space Mission Analysis and Design (p. 141), by J. R. Wertz, et al., 1992. Copyright 1992 by Microcosm, Inc.

3.3.3 IGP4

The next routine, IGP4, is a simplification of the Air Force General Perturbation Theory. This particular algorithm differentiates itself from AFGP4 by replacing the extensive drag model found in AFGP4 with a simplified one instead. The details of the simplified drag model can be found in (Lane & Hoots, 1979, pp. 25-33). What it comes down to, is that all values *except* linear variations (also known as *secular variations*) in the orbital elements and periodic terms of "important magnitude" (Figure 3-3) are dropped (Lane & Hoots, 1979, p. 25). This means that from the extensive drag model, the drag terms that do not have a major contribution to the motion of the satellite are disregarded.

In addition to the simplified drag periodics, the propagated *mean* mean anomaly, argument of perigee, and right ascension of the ascending node are no longer iteratively found, but instead are represented by analytical expressions (Lane & Hoots, 1979). Furthermore, the Brouwer geopotential model with Lyddane's modification is also carried over from AFGP4. These two

simplification do indeed speed up the calculation routine from AFGP4, but do it at the expense of accuracy.

The calculation routine for IGP4 is the same as AFGP4 (Section 3.3.2) with steps 4 and 5 being replaced with the simplified equations found in *Spacetrack Report Nr. 2* (Lane & Hoots, 1979, pp. 25-38). The differences between AFGP4, IGP4, and SGP4 were slight for most objects. Unfortunately, "IGP-4 and AFGP-4 have been eliminated as functioning programs" due to the limited hardware capacity and processing limitations of the two Honeywell 6080 computers (Figure 3-4) the Space Computation Center used in the 1970's (Staats, 1978).



Figure 3-4. The Honeywell 6080 Computer. Adapted from *Consoles, Computers and Code* on Pinterest, by T. Killingsworth, Retrieved from <http://pinterest.com/pin/463237511649565415/>. Copyright 2016 by T. Killingsworth.

Although, AFGP4 and IGP4 were designed for efficient performance, the decision to use SGP4 was ultimately due to "limited computer hardware capacity" (Staats, 1978, pp. 17-18). Thus, SGP4 was used and turned into the *de facto* standard that is still in use today.

3.3.4 Simplified General Perturbation Theory Nr. 4

The Simplified General Perturbation Nr. 4 model (SGP4), is another simplification of the IGP4 model, which means that it happens to also be another simplification of the AFGP4 model. Based off the works by (Lane M. H., 1965), and (Lane & Crawford, 1969), this Brouwer-based model (AIG, 2016) served as a replacement for the other orbital models: SGP, AFGP4, and IGP4. The primary difference between the older SGP and SGP4 was in the formulation of mean motion and the atmospheric drag representation.

Lane and Cranford's main objective was to develop a theory that would improve upon the orbit propagation of high-drag satellites while keeping computational time down to a minimum (AIG, 2016).

Not only were the simplified drag periodics of IGP4 taken into account, but also includes simplified expressions for Earth's secular, long-term, and short-term geopotentials; namely, the variables that involve J_2 , J_3 , and J_4 (Herriges, 1988, p. 47). Furthermore, the geopotential simplification also assumes that the eccentricity of the satellite is small (nearly circular), and the drag forces of satellite, with a close-to-zero inclination experience the same forces as satellites with larger inclinations (Lane & Hoots, 1979, pp. 39-51). These simplifications ultimately contribute to an initial positioning error of one km and grow in error from one to three kilometers per day (Vallado, Crawford, Hujesak, & Kelso, 2006, p. 33).

The development of the SGP4 model is thoroughly described in *General Perturbations Theories Derived from the 1965 Lane Drag Theory* (Lane & Hoots, 1979, pp. 47-51), *Models for Propagation of NORAD Element Sets* (Hoots & Roehrich, 1980, pp. 10-30), and *Revisiting Spacetrack Report #3* (Vallado, Crawford, Hujesak, & Kelso, 2006). Therefore, the development of this model will not be described here. SGP4 can be broken down into the following steps (Hoots & Roehrich, 1980, pp. 10-30, 58):

1. Obtain the orbital elements from a TLE and determine the time of interest for propagating the satellite.
2. Recover the mean motion and semi-major axis from the TLE.
3. Determine if the perigee of the satellite is less than 220 kilometers and initialize common and time-variant variables, and drag terms.
4. Determine if the satellite is considered a *deep-space object*. If so, all time independent quantities are calculated and flags are set depending upon whether the orbit is synchronous and/or experiences resonance effects.

5. Modify the calculated variables to include secular gravity and atmospheric drag effects.
6. If the satellite is a deep-space object, "the appropriate deep-space secular and long-period resonance effects" are added to the elements.
7. If the satellite is a deep-space object, add to the calculated quantities the gravitational acceleration effects caused by the moon and sun.
8. Iteratively solve Kepler's equation to a desired accuracy.
9. Calculate the short-period periodics of the satellite (Figure 3-3).
10. Calculate the position and velocity vectors at the new time of interest.

3.3.5 Simplified General Perturbation Theory Nr. 8

Simplified General Perturbation Theory Nr. 8 (SGP8) was officially introduced to the public for the first time in *Spacetrack Report Nr. 3*. This occurred alongside the SGP and SGP4/SDP4 orbital propagation models.

The difference in the distance and velocity vectors between the SGP4 and SGP8 models is relatively small (with distance variations ranging from approximately 20 to 220 meters after propagating an orbit for a day²⁹). Pretty much, it came down to two alterations to the SGP4 code: modeling trajectories of low-altitude satellites that are about to re-enter the atmosphere (Vallado, Crawford, Hujak, & Kelso, 2006, p. 2) and in how the equations dealing with atmospheric and gravitational variations are integrated.

With respect to modeling low-altitude satellites, the SGP8 model takes into account the actual ballistics coefficient, B , of the satellite instead of the pseudo drag term, B^* , that is found in SGP4. Furthermore, if the ballistics coefficient is small, and hence a low drag term³⁰, the drag equations are then "truncated to linear variation[s] in [the] mean motion and quadratic variation[s] in [the] mean anomaly." This means that since the drag term is small, short- and long-term periodics are so small, that accounting for them does not contribute much to the result. This modification not only speeds up calculations, but also allows for more

²⁹ Found by taking the difference in the magnitude of the distance vector for 0 and 1440 minutes in *Spacetrack Report Nr. 3* (Hoots & Roehrich, 1980, pp. 81, 83).

³⁰ $\frac{n}{n_0}$ less than 1.5E-6 per minute (Hoots & Roehrich, 1980, p. 37).

accurate predictions of low-altitude satellites that are about to decay and re-enter Earth's atmosphere.

The second modification is in how the differential equations dealing with gravitational and atmospheric effects in *An Improved Analytical Drag Theory for the Artificial Satellite Problem* (Lane & Crawford, 1969) are integrated (Hoots & Roehrich, 1980, p. 1)

The steps to go from TLE to position vectors are the same as presented in Section 3.3.4 (with the only differences being with the drag term presented in step 3 and with the gravity and drag effect in step 5).

Table 3-2. Computational Speed of Propagators in 1988. Adapted from *Spacetrack Report No. 3: Models for Propagation of NORAD Element Sets* (p. 85), by F. R. Hoots and R. L. Roehrich, 1988, Copyright 1988 by US Department of Defense.

PROGRAM SYMBOL	CPU TIME PER CALL (MILLISECONDS)
SGP	3.5
SGP4	4.4
SGP8	4.0
SDP4	8.7
SDP8	8.6

It is worth noting that back in 1980, time and consideration was given in replacing SGP4 by SGP8 as the standard satellite model. The elements sets that would be generated by SGP8 would still be compatible with the previously mentioned propagators (Hoots & Roehrich, 1980, p. 2). However, 26 years later, Vallado, Crawford, Hujsak and Kelso noted that "there is [still] no evidence to suggest that SGP8/SDP8 was implemented for operational TLE formation." Thus, why SGP4 remains the *de facto* standard is still a mystery even though a newer and faster (Table 3-2) closed-form propagator exists today (Vallado, Crawford, Hujsak, & Kelso, 2006).

3.4 Conclusion

In this chapter, the different methods and techniques that are used for orbit propagation were explored. Orbit propagators have evolved over the years since their first introduction in the early 1950s. Since then, there have been two main methods of calculating the precise orbit of a satellite. Whether by numerical integration or closed-form solutions, both techniques take the same TLE and give

the satellite's position and velocity vector at any given point in time, even though what happens in the middle varies extensively.

Bringing everything together, the characteristic differences between the different closed-form solutions are found in Table 3-3. Furthermore, the different two methods of propagating an orbit are summarized in the following two ordered lists:

Numerical Integration

1. Each individual force that is acting upon the satellite that is of interest is evaluated.
2. These forces are used to determine the accelerations experienced on the spacecraft.
3. The satellite's position and velocity vectors are determined by integrating the calculated accelerations using very small time-steps.
4. This process repeats until the desired time is reached.

Closed Form Solutions

1. Obtain the orbital elements from a TLE and determine the time of interest for propagating the satellite.
2. Initialize common variables.
3. Calculate time-dependent quantities.
4. Modify these variables to include secular, long-period, and short-period time-dependent perturbations
5. Iteratively solve Kepler's equation to a desired accuracy.
6. Calculate the position and velocity vectors at the new time of interest.

One major problem for predicting the location of a satellite is that as a satellite is propagated forward in time further away from its epoch, errors increase. Therefore, some sort of mechanism needs to be put in place to minimize these errors. This mechanism allows for a more precise and accurate orbital position and velocity vector estimate. In the following chapter, these mechanisms are explored.

Table 3-3. Differences among Common Orbital Propagators. Adapted by Paul Schattenberg from "Revisiting Spacetrack Report #3", by D. A. Vallado, P. Crawford, R. Hujsak, and T. S. Kelso, *American Institute of Aeronautics and Astronautics*, 2006, Copyright 2006 by AIAA/AAS.

MODEL	CHARACTERISTICS
SGP	<ul style="list-style-type: none"> • Used for near-Earth satellites • Simplified gravitational model • The drag effect on mean motion is linear in time. • The drag effect on the eccentricity keeps perigee height constant. • If the satellite is a near-Earth satellite, drag effects resemble that of the SGP4 model, else they resemble the drag effects of the SDP4 model.
SGP4/SDP4	<ul style="list-style-type: none"> • Used for Deep-Space and near-Earth satellites • Takes gravitational effects of the Moon and Sun into account • Uses terrestrial Earth harmonics for satellites with large periods • Used for generating the NORAD two-line elements sets
SGP8/SDP8	<ul style="list-style-type: none"> • Used for Deep-Space and near-Earth satellites • Improved algorithms for orbital decay • Uses an extensive analytical Earth-gravitational and atmospheric model • Takes gravitational effects of the Moon and Sun into account • Uses terrestrial Earth harmonics for satellites with large periods • Uses the same gravitational and atmospheric models of SGP4/SDP4, but by using a very different analytical approach • Uses the ballistic coefficient in the drag equation instead of the pseudo drag term used in the SGP4/SDP4 model

Chapter 4 Modern Orbit Determination Techniques

“Imagination will often carry us to worlds that never were. But without it we go nowhere.”

- Carl Sagan

4.1 Background Information

Orbit determination is the computational method or process used to determine the position and velocity of the spacecraft and the spacecraft's orbital elements. Carl Gauss first proposed a solution to this problem in 1801 when astronomers wanted to determine the orbit of a newly discovered asteroid, Ceres. His solution, published a few years later, utilized three angles and his *least-squares technique* to fit a curve through these three points in space (Vetter, 2007, p. 241). His method was applicable to objects primarily orbiting our sun; however, the solution could also be used to provide a rough estimate for the initial determination of a satellite's orbit about Earth.

The need for orbit determination of Earth-orbiting satellites did not necessarily arise until the launch of Sputnik in October of 1957. In the early days of space program, RADAR and optical observations from cameras and cinetheodolite³¹ provided orbit determination data (Table 4-1), but their accuracies were only to a few kilometers (Vetter, 2007, pp. 241-242). Later, by using a mixture of RADAR and optical measurements, positional uncertainty dropped to

³¹ A photographic instrument used to collect trajectory data.

about 500 meters. In the late 1960s, laser-ranging systems equipped with reflectors were used to track satellites. This method works by using short pulses of light and measures the two-way time-of-flight between when the beam and the satellite to determine the distance to the satellite. Initially, this method was able to provide the same information as RADAR and optical measurements, but could determine the distance to the satellite with 5 to 10 meters accuracy (Vetter, 2007, p. 242). With advancements in technology, the altitude of the orbit of a satellite can now be determined to less than 5 centimeters; however, the cross-track and along-track uncertainties of the satellite's location remain (Vallado & Agapov, 2010, p. 3). According to Wertz and et. al., cross-track error is directly related to an error in measuring the inclination and right ascension of the ascending node of the satellite (Wertz, Collins, Dawson, Hönigsmann, & Potterveld, 1997, p. 270).

Table 4-1. Observational Data Types Used for Orbit Determination. Adapted from "Fifty Year of Orbit Determination" by J. R. Vetter, 2007, Johns Hopkins APL Technical Digest, 27, p. 247. Copyright 2007 by J. R. Vetter.

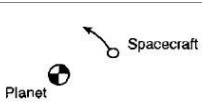
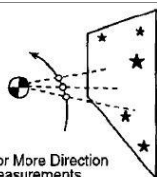
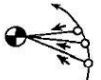
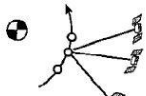
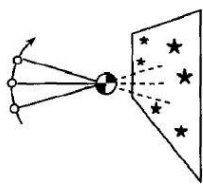
OBSERVATIONAL DATA TYPE	SOURCE
Azimuth and Elevation Angles, Slant Range	Passive or Active Radar
Right Ascension and Declination	Baker-Nunn Cameras, Telescopes, Binoculars, Visual Sightings, Big Dish RADAR Telescopes, Cinetheodolites
Azimuth	Direction Finders
TCA	Radars, Radio Receivers
Range, Angles, and Range-Rate	Special Doppler Radars
Space-based Observations	Onboard Instruments
Pseudo-Range, and Carrier Phase	GPS

Today, the orbit determination process is generally approached by using some combination of onboard and/or ground-based measurements. Table 4-1 lists the different data types commonly used for orbit determination and their source. Because the satellite is influenced by many non-linear forces³², measurements must be taken periodically in order to determine accurately the location of the spacecraft. Multiple methods exist for taking these measurements. However,

³² Non-gravitational interactions, third-body interactions, non-spherical mass distributions, and relativistic effects

some methods are better suited for other applications, and thus produce slightly different results in obtaining the orbital elements of a satellite. The most common methods for determining these elements are found in Table 4-2.

Table 4-2. Common Measurement Sets for Orbit Determination. Adapted from *Mission Geometry; Orbit and Constellation Design and Management* (p. 105-106), by J. R. Wertz, et al., 2001. Copyright 2001 by Microcosm, Inc.

DATA SET	TYPICAL APPLICATION	
1	Injection from the Launch Vehicle; Results of a Maneuver	
2	Traditionally Used for Comets and Asteroids	
3	Used in Ground Tracking Systems	
4	GPS-Based Orbit Determination	
5	Optical Autonomous Navigation	

In the following sections, a general overview of the orbit determination problem and process will be discussed. These methods allow for the calculation of the position and velocity vector of the satellite orbiting Earth.

4.2 The Orbit Determination Problem

Simply stated, an orbit determination problem can be expressed as

$$\ddot{\vec{r}} = -\frac{GM}{r^3}\vec{r} + f_G + f_{NG} \quad 4-1$$

where the term f_G and f_{NG} contain the sum of the gravitational and non-gravitational accelerations acting on the satellite, respectively. Gravitational accelerations include perturbations on the satellite that arise from Earth's tides, and relativistic effects. Non-gravitational effects include acceleration changes due to atmospheric drag, solar and Earth radiation pressure, and accelerations caused by thermal radiation. The satellite's state vector, r , includes acceleration effects caused by Earth's gravity field and drag (Vetter, 2007, p. 246). However, the estimates will always differ from the actual location of the spacecraft due to random, systematic, and computational errors³³ in the observation data and instruments used, and from the mathematical representations of the various types of external forces on the satellite.

4.3 The Orbit Determination Process

The orbit determination process is a multi-step process where the orbital elements are constantly being updated while the satellite remains in orbit. This is due to many non-linear effects and accelerations that the satellite will experience during its lifetime.

It is a trivial task to convert the position and velocity vectors of the satellite into TLEs (Bate, Mueller, & White, 1972, pp. 58-71). However, the computationally intensive process lies within the accurate determination of these vectors. In order to achieve accurate positional estimates of the satellite, an iterative process in refining the initial orbital elements must be done between the observed location of the satellite in space and the ground station. This process is summarized in the following steps³⁴ and in part of Figure 4-1:

³³ First-order vs. Second-order solutions

³⁴ Steps 3 to 9 happen to be shown in Figure 4-1.

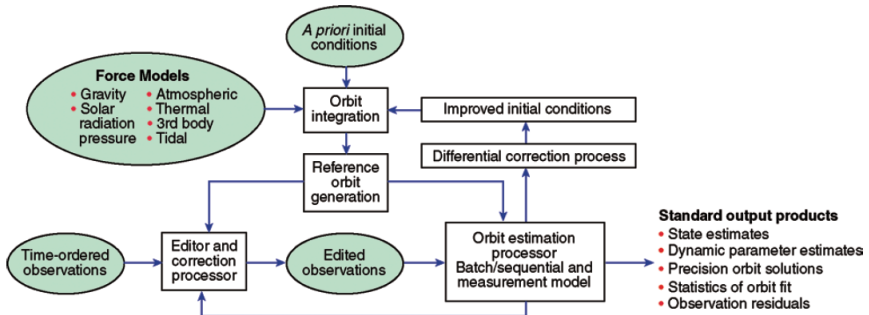


Figure 4-1. The Orbit Determination Process. Adapted from "Fifty Year of Orbit Determination" by J. R. Vetter, 2007, *Johns Hopkins APL Technical Digest*, 27, p. 245. Copyright 2007 by J. R. Vetter.

1. Take sighting observations of the satellite.
2. Convert these observations into position, \mathbf{r} , and velocity, \mathbf{v} , vectors and the initial TLE. These two vectors are known as the *a priori* initial conditions in Figure 4-1.
3. Using a force model of the Earth, determine the orbit of the satellite forward in time.
4. With this information, determine the time-ordered observational guesses of the satellite.
5. If a "downrange station can get another 'six-dimensional fix' on the satellite," skip to step 9.
6. If step 5 is not possible, take at least six observations of a particular orbital property the satellite and determine the errors and residuals associated between the time-ordered observational guesses of the satellite and the new sighting observations.
7. Use the differential correction methods outlined in *Fundamentals of Astrodynamics* (Bate, Mueller, & White, 1972, pp. 122-131) to improve upon the initial orbit estimation.
8. Using the improved orbit estimation data, iterate steps 3 through 6 until the residuals are either zero or are within an acceptable range.
9. Once the residuals are small enough or a new "six-dimensional fix" on the satellite was obtained, compute new *corrected* orbital

elements³⁵ and put this in TLE format. This new TLE is to be used for future orbit estimations.

10. If smoothing of the elements is necessary, average the orbital elements over some period of time (Bate, Mueller, & White, 1972, p. 122).³⁶

There are multiple ways step 1 and 2 can be achieved. Common methods employ the use of RADAR, visual sightings, radio receivers, lasers, and/or on-board instruments (Table 4-2). Some of the force models of step 3 are outlined in Chapter 3 with "all TLE data [being] generated by SGP4" (Vallado, Crawford, Hujsak, & Kelso, 2006, p. 31).

In the parts that follow, various ways in how the position and velocity vector of the satellite can be determined will be discussed.

4.3.1 A Single RADAR Observation

A single radar site is capable of measuring the distance, ρ , and the azimuth and elevation of the satellite from the ground station. With this information alone, the vector $\boldsymbol{\rho}$ can be calculated (Figure 4-2) and thus the position of the satellite relative to the geocentric frame can be determined, \mathbf{r} .

This vector is expressed as the position vector,

$$\boldsymbol{\rho} = \langle \rho_S \mathbf{S}, \rho_E \mathbf{E}, \rho_Z \mathbf{Z} \rangle \quad 4-2$$

where the subscripts denote positive values in the direction of south, east, and z is the vertical up to the satellite. The individual values of ρ are expressed as

$$\rho_S = -\rho \cos El \cos Az \quad 4-3$$

$$\rho_E = \rho \cos El \sin Az \quad 4-4$$

$$\rho_Z = \rho \sin El \quad 4-5$$

Thus, the relationship between $\boldsymbol{\rho}$ and \mathbf{r} can be expressed as

$$\mathbf{r} = \boldsymbol{\rho} + \mathbf{R} \quad 4-6$$

³⁵ This gives the user true time-varying orbital elements that include all periodic and secular effects (Vallado & McClain, 2004, p. 574).

³⁶ Useful for mission planning purposes (Vallado & McClain, 2004, p. 574).

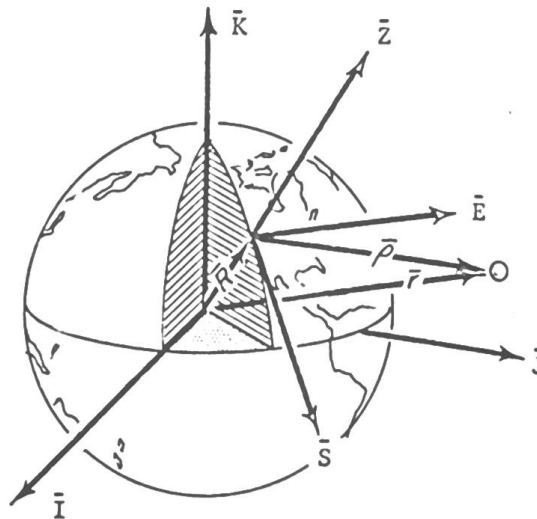


Figure 4-2. Ground Station and Satellite Vectors. Adapted from "Fundamentals of Astrodynamics" by Bate, Mueller, and White, 1972, p. 86. Copyright 1971 by Dover Publications, Inc.

where \mathbf{R} is the geocentric position vector between the center of the Earth and the location of the observation site³⁷, and \mathbf{p} and \mathbf{r} are as previously defined.

If the radar is capable of detecting a Doppler shift of the returning echo and the rate-of-change of the azimuth and elevation angles, the velocity vector, \mathbf{v} , of the satellite can also be determined by differentiating equations 4-3 to 4-6. If this information is not available, the Lagrange interpolation formula found in *Fundamentals of Astrodynamics* (Bate, Mueller, & White, 1972, p. 119) can also be used to determine the velocity of the satellite.

A detailed explanation of using a single radar site for observations can be found in sections 2.7 and 2.8 of *Fundamentals of Astrodynamics* (Bate, Mueller, & White, 1972, pp. 83-101).

4.3.2 Multiple Optical Sightings

A more classical approach to the orbit determination problem utilizes ground-based observations from cameras. This method is more involved than using RADAR observations because the only variables that are shared between

³⁷ Due to the Earth's rotation, this position vector changes as a function of time.

optical sightings and RADAR observations are the azimuth and elevation of the satellite at a particular point in time. However, what makes this process of particular interest is that the cameras provide pointing accuracies and resolutions that exceed those of RADAR sites (Bate, Mueller, & White, 1972, p. 117) (Vetter, 2007, p. 241).

Because of being able to only obtain azimuth and elevation data, all calculations need to be normalized, and an iterative process needs to be performed on an eight-order equation until convergence. Once this equation converges, determining the position and velocity vector for the satellite at one of the measured times becomes a trivial task.

The process of using multiple optical sightings is explained in detail in section 2.11 of *Fundamentals of Astrodynamics* (Bate, Mueller, & White, 1972, pp. 117-122); however, a brief summary will be presented below.

In order to use this method, at least three sets of information are needed: the azimuth, elevation, and the time the measurement was taken. With this information, the first step is to convert the azimuth and elevation of the satellite sighting into the equatorial coordinate system (Figure 4-3) (Meeus, 2009, pp. 87-88, 91-94).

From here, three separate unit vectors, \mathbf{L} , can be constructed for all three observations. The main equation is,

$$\mathbf{r} = \rho \mathbf{L} + \mathbf{R} \quad 4-7$$

where \mathbf{r} , ρ , \mathbf{R} , and \mathbf{L} are as previously defined. This equation is quite similar to equation 4-6 presented in the previous section. The main difference come in the fact that ρ is now split up into two components, ρ and \mathbf{L} since the distance to the satellite is unknown. Furthermore, the right ascension and declination of the observation is used instead of azimuth and elevation. Thus, vector \mathbf{L} of equation 4-6 becomes,

$$\mathbf{L}_i = \begin{bmatrix} \cos \delta_i \cos \alpha_i \\ \cos \delta_i \sin \alpha_i \\ \sin \delta_i \end{bmatrix}. \quad 4-8$$

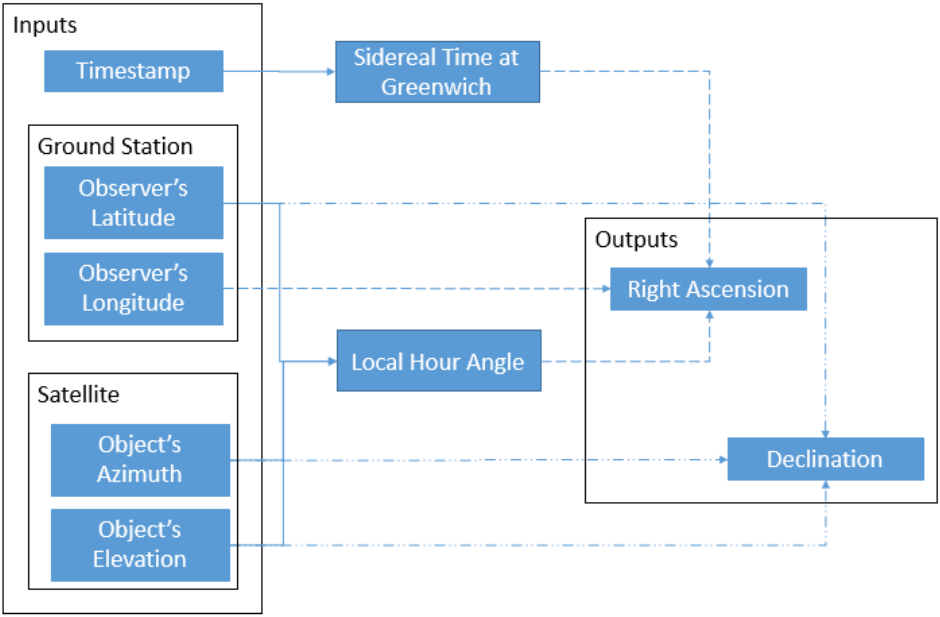


Figure 4-3. Transformation of Coordinate Systems. *Note.* This process needs to be carried out for each set of observations.

The next step is to take Lagrange's interpolation formula (Equation 4-9) for n -number of sightings and differentiate the resulting equation two times to determine the first and second derivative of L .

$$L(t) = \sum_{j=1}^n L_j \prod_{\substack{k=1 \\ k \neq j}}^n \frac{t - t_j}{t_j - t_k} \quad 4-9$$

By taking the second derivative of equation 4-7,

$$\ddot{\mathbf{r}} = \ddot{\rho} \mathbf{L} + 2\dot{\rho} \dot{\mathbf{L}} + \rho \ddot{\mathbf{L}} + \ddot{\mathbf{R}} \quad 4-10$$

which can be further simplified using the relationship,

$$\ddot{\mathbf{r}} = -\mu \frac{\mathbf{r}}{r^3} \quad 4-11$$

to obtain,

$$\mathbf{L}\ddot{\rho} + 2\dot{\mathbf{L}}\dot{\rho} + \left(\ddot{\mathbf{L}} + \mu\frac{\mathbf{L}}{r^3}\right)\rho = -\left(\ddot{\mathbf{R}} + \mu\frac{\mathbf{R}}{r^3}\right). \quad 4-12$$

Applying Cramer's rule to equation 4-12 and solving for ρ , the following expression is obtained,

$$\rho = \frac{-2D_1}{D} - \frac{2\mu D_2}{r^3 D} \quad 4-13$$

where D , D_1 , and D_2 are the determinates of the matrices found in *Fundamentals of Astrodynamics* (Bate, Mueller, & White, 1972, pp. 120-121).

By dotting equation 4-7 onto itself (Equation 4-14), and substituting equation 4-13 into this equation, you can ultimately arrive at an expression that can be iterated to solve for r , and thus allowing for ρ to be solved for.

$$r^2 = \rho^2 + 2\rho\mathbf{L} \cdot \mathbf{R} + R^2 \quad 4-14$$

With this value of ρ , the position vector of the satellite can be finally determined using equation 4-7. Similarly, by applying Cramer's rule once more to equation 4-12 and solving for the first derivative of ρ , the velocity vector, \mathbf{v} , can be determined. With \mathbf{r} and \mathbf{v} now known, the *a priori* initial conditions as shown in Figure 4-1 are found and now the orbital elements of the satellite can be determined.

4.3.3 The Gauss Problem and Solution Techniques

The last of the methods to determine the orbit of a satellite from a ground station is called the *Gauss Problem*. This method was first proposed by Carl Gauss in the early 1800s. Back then, it was a much more complex problem than it is today, since position vectors of the satellite can easily be obtained instantaneously from RADAR. This method is of particular interest because not only is it applicable to orbits of spacecraft, but also serves as part of the solution to rendezvous and docking of spacecraft.

The Gauss problem and a few solution techniques are well documented and explained in *Fundamentals of Astrodynamics* (Bate, Mueller, & White, 1972, pp. 228-258). Nevertheless, this problem will be examined from a top-down

perspective and the different solution techniques that are currently implemented will be briefly mentioned.

In order for the Gauss problem to be of any use, three pieces of information are needed. These are the two position vectors of the satellite (\mathbf{r}_1 and \mathbf{r}_2) and the elapsed time between these two observations, t . With this information alone, the angle between these two vectors (\mathbf{r}_1 and \mathbf{r}_2), Δv , can be determined.

$$\mathbf{r}_1 \cdot \mathbf{r}_2 = r_1 r_2 \cos \Delta v \quad 4-15$$

Ultimately, the two velocity vectors of the satellite (\mathbf{v}_1 and \mathbf{v}_2) can be determined from the following process, and from that, the six orbital elements are found (Schattenberg, 2014). A full derivation of the four resulting equations presented below can be found in *Fundamentals of Astrodynamics* (Bate, Mueller, & White, 1972, pp. 193-203, 212-222):

$$f = 1 - \frac{r_2}{p}(1 - \cos \Delta v) = 1 - \frac{a}{r_1}(1 - \cos \Delta E) \quad 4-16$$

$$g = \frac{r_1 r_2}{\sqrt{\mu p}} \sin \Delta v = t - (\Delta E - \sin \Delta E) \sqrt{\frac{a^3}{\mu}} \quad 4-17$$

$$\dot{f} = \sqrt{\frac{\mu}{p}} \tan \Delta v \left(\frac{1 - \cos \Delta v}{p} - \frac{1}{r_1} - \frac{1}{r_2} \right) = -\frac{\sqrt{\mu a}}{r_1 r_2}. \quad 4-18$$

$$\dot{g} = 1 - \frac{r_1}{p}(1 - \cos \Delta v) = 1 - \frac{a}{r_1}(1 - \cos \Delta E) \quad 4-19$$

These equations consist of three knowns (r_1 , r_2 , and t), three unknowns (p , a , and ΔE), and one constant, μ ³⁸. These four variables are then used to solve the following two equations for \mathbf{v}_1 (Equation 4-20) and \mathbf{v}_2 (Equation 4-21):

$$\mathbf{r}_2 = f\mathbf{r}_1 + g\mathbf{v}_1 \quad 4-20$$

$$\mathbf{v}_2 = \dot{f}\mathbf{r}_1 + \dot{g}\mathbf{v}_1 \quad 4-21$$

³⁸ As defined in Appendix A.

There are multiple solution techniques presented in *Fundamentals of Astrodynamics* (Bate, Mueller, & White, 1972, pp. 228-258) to solve for the three unknown variables (p , a , and ΔE). Thus forming the basis on how to approach and solve for f , g , and their derivatives. The different solution techniques include *The p-Iteration Method* (pp. 241-251), *The Method of Universal Variables* (pp. 231-236), and *The f and g Series Method* (pp. 251-258).

In short, what these three methods result in is making a guess for one of the variables, solving for the remaining two unknown, and comparing the calculated time-of-flight from equation 4-26 with the observed time-of-flight between the two measurements. If the two time-of-flights fall within an acceptable margin of error, the calculated variables are then used in equation 4-20 and 4-21 along with the two position vectors of the satellite to determine the TLE of the observed satellite.

4.3.4 On-Board Instruments

Instrumentation can provide many interesting data for orbit determination either *directly* or *indirectly*. These two words mean that a satellite is either capable of determining its Keplerian elements from sensor data *directly* or it uses the sensor data to derive other values that can then be useful to determine Keplerian elements *indirectly*. An example of an indirect method would be to use solar panel voltages to be able to deduce the vector from the spacecraft to the Sun. Mainly, literature points to techniques that use data from magnetometers and sun sensor data for orbit determination. Therefore, this is what will be examined in this subsection.

Before looking at this method, it is worth mentioning some contributors to on-board orbit determination errors. These contributors come from clock synchronization, how the CPU handles arithmetic, and the computational time required (Bowen, 2009, p. 62). The largest potential source of error is with time synchronization (Vallado & Agapov, 2010, p. 3). This is important for LEO satellites because if the on-board clock were to be off by just *one*-second, the spacecraft could experience a positioning error upwards of eight kilometers.

One of such process for on-board orbit determination uses a three-axis magnetometer and a two-axis sun sensor. This method and all its equations are outlined in detail in the report titled *Autonomous Low-Earth-Orbit Determination from Magnetometer and Sun Sensor Data* (Psiaki, 1999). However, what it comes down to is using the magnetometer and sun sensor measurements to form a p

estimation vector that contains the Keplerian elements of the satellite (Equation 4-22).

$$\mathbf{p} = [M_0, M_1, M_2, e, \omega_0, \lambda_0, i, b_x, b_y, b_z, q_1^0, q_1^1, s_1^1, \dot{q}_1^0, \dot{q}_1^1, \dot{s}_1^1, \dot{g}_1^0, \dot{g}_1^1, \dot{h}_1^1, \Delta g_1^0, \Delta g_1^1, \Delta h_1^1, \Delta g_2^0, \Delta g_2^1, \Delta h_2^1, \Delta g_2^2, \Delta h_2^2, \Delta g_3^0, \dots, \Delta h_N^N]^T \quad 4-22$$

Here, the first seven quantities are the items of interest. These are the satellite's mean anomaly, mean motion, mean motion divided by two, eccentricity, argument of perigee, right ascension of the ascending node, and the inclination. The other quantities are the magnetometer bias (elements 8 to 10), and the corrections to the Earth's magnetic field (element 11 and up) (Psiaki, 1999, p. 297).

This particular method uses a batch filter to estimate the vector \mathbf{p} by determining the values of \mathbf{p} that minimize following two equations:

$$e_{1(k)} = \frac{1}{\sigma_B} [y_{1mod}(\Delta t_k; \mathbf{p}) - y_{1mes(k)}(\mathbf{p})] \quad 4-23$$

$$e_{2(k)} = \frac{1}{\sigma_{y2(k)}} [y_{2mod}(\Delta t_k; \mathbf{p}) - y_{2mes(k)}(\mathbf{p})] \quad 4-24$$

The variables are as defined in *Autonomous Low-Earth-Orbit Determination from Magnetometer and Sun Sensor Data* (Psiaki, 1999). The variables y_1 and y_2 are pseudo measurements that are dependent upon the magnetic field and sun vector. The variables y_{1mod} and y_{2mod} are the iteratively found pseudo measurements that minimize equations 4-23 and 4-24.

This \mathbf{p} estimation vector is then compared to simplified models of the Earth's magnetic field³⁹ and the positing vectors of the Sun. From looking up values found in the simplified magnetic field model on-board the satellite, the statistical estimation and probability of where the satellite is along with its orbital elements can be determined (Psiaki, 1999). Results of this method for the accuracy that can be determined using this method are found in Figure 4-4.

³⁹ Usually the most up-to-date IGRF model (Bowen, 2009, p. 26). In Bowen's report, the IGRF model was "used to develop less computationally demanding models."

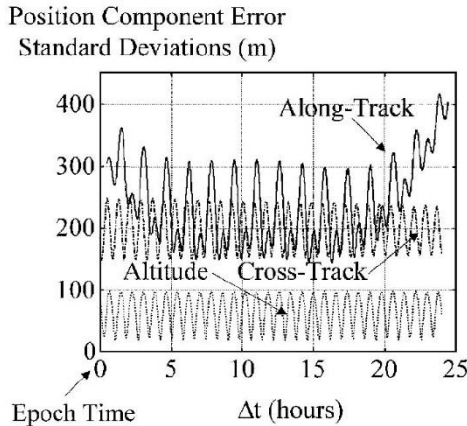


Figure 4-4. Positioning Estimation-Error Resulting from Magnetometers and Sun Sensor data. Adapted from "Autonomous Low-Earth-Orbit Determination from Magnetometer and Sun Sensor Data" by M. Psiaki, 1999, *Journal of Guidance, Control, and Dynamics*, 27, Nr. 2, p. 302. Copyright 1999 by M. Psiaki.

4.4 The Differential Correction Process

The differential correction process is a process that is used to improve the TLEs of a satellite when a *six-dimensional fix*⁴⁰ on the satellite is not possible. This means that a downrange ground station is unable to measure six independent variables to determine and improve the initial orbit estimation of a satellite. In section 4.3, the assumption is made that either the initial station or downrange station is capable of determining one of the following six sets of variables:

- Az , El , ρ , and their rates at a specific point in time,
- Az , El , ρ , and their timestamp for two separate points in time,
- Az , and El and their timestamp for three separate points in time⁴¹, and
- α and δ for three points in time.

If these six sets of variables are available, the TLE of the satellite can be improved by taking an average of the newly generated TLEs with the previously

⁴⁰ Assuming the downrange ground station is interested in determining the two three-component r and v -vectors. This is usually the case, as it is these vectors that are used to generate TLEs.

⁴¹ Used in calculating the satellites α and δ .

generated TLEs for that satellite (Bate, Mueller, & White, 1972, p. 122) (Vallado & McClain, 2004, p. 574).

However, if a downrange ground station cannot fully measure any complete set, but can measure at least one particular variable, this information can still be used in improving upon the previously generated TLE. This technique is called *Differential Correction* and it is all about using the residuals between measured and theoretical data to improve upon the generated TLE.

In order for this method to work, theoretical pass prediction information such as where the satellite should be in the sky at a certain time, and the measured parameter at that time is needed. This allows a six-dimensional matrix for correcting the initial orbit estimation to be formed and solved. By analogy, differential correction applies a Newton iteration scheme to the initial \mathbf{r} and \mathbf{v} -vectors, but in six dimensions simultaneously.

The differential correction method presented in *Fundamentals of Astrodynamics* is more involved. Not only does it use more matrix multiplication, but also briefly outlines an intermediate step to take when no unique solution exists. The method presented below is a simplified version of the one found in *Fundamentals of Astrodynamics* (Bate, Mueller, & White, 1972, pp. 122-131). More details of this method can also be found in Chapter 10 of *Fundamentals of Astrodynamics and Applications* (Vallado D. A., 2007).

Keeping with the newton iteration analogy, the first step is to expand the Taylor series polynomial out to the first derivative:

$$\begin{aligned} f(x_{i+1}) &= \sum_{n=0}^{\infty} \frac{f^n(x_i)}{n!} (x_{i+1} - x_i)^n \\ &= f(x_i) + f'(x_i)(x_{i+1} - x_i). \end{aligned} \quad 4-25$$

Next, solve for $f(x_{i+1}) - f(x_i)$: the characteristic equation that is used for setting up six-dimensional matrix for differential correction.

$$f(x_{i+1}) - f(x_i) = f'(x_i)(x_{i+1} - x_i) \quad 4-26$$

On the left-hand side of the equation, $f(x_{i+1})$ is synonymous to the downrange observed parameter and $f(x_i)$ is the theoretical observed value. The right hand-side of the equation contains two unknowns:

- $f'(x_i)$ - A partial derivative of the measured parameter with respect to one of the *a priori* initial conditions, and

- $(x_{i+1} - x_i)$ - The *a priori* initial condition correction factor.

Both of these variables can be solved for numerically. For the sake of this example, $f(x_{i+1}) - f(x_i)$ is expressed as Δf_i . Equation 4-26 is then expressed as a six-dimensional matrix,

$$\begin{bmatrix} \Delta f_1 \\ \Delta f_2 \\ \Delta f_3 \\ \Delta f_4 \\ \Delta f_5 \\ \Delta f_6 \end{bmatrix} = \begin{bmatrix} f'(x_1) & f'(x_1) & f'(x_1) & f'(x_1) & f'(x_1) & f'(x_1) \\ f'(x_2) & f'(x_2) & f'(x_2) & f'(x_2) & f'(x_2) & f'(x_2) \\ f'(x_3) & f'(x_3) & f'(x_3) & f'(x_3) & f'(x_3) & f'(x_3) \\ f'(x_4) & f'(x_4) & f'(x_4) & f'(x_4) & f'(x_4) & f'(x_4) \\ f'(x_5) & f'(x_5) & f'(x_5) & f'(x_5) & f'(x_5) & f'(x_5) \\ f'(x_6) & f'(x_6) & f'(x_6) & f'(x_6) & f'(x_6) & f'(x_6) \end{bmatrix} \begin{bmatrix} \Delta r_i \\ \Delta r_j \\ \Delta r_k \\ \Delta v_i \\ \Delta v_j \\ \Delta v_k \end{bmatrix} \quad 4-27$$

This equation might look scary at first, as there are 36 unknown partial derivatives. However, these 36 individual derivatives can be solved numerically with an initial guess for the denominator of equation 4-28 and by updating these 36 matrix elements using new residuals with each successive iteration.

$$f'(x_i) = \frac{df}{dx_i} = \frac{f(x_{i+1}) - f(x_i)}{\Delta x_i} \quad 4-28$$

What is of particular interest in equation 4-27 is the vector containing Δr and Δv . These individual six components allow for a correction factor to the *a priori* initial conditions to be formed after each successive iteration to improve upon the TLE using what the downrange ground station observed.

The differential correction process is summarized as follows:

1. Determine the residuals of one of the observation parameters, Δf_i .
2. Provide an initial small-value estimate to the denominator in equation 4-28 for each of the six columns. After the first iteration, use the calculated values for Δr and Δv obtained in step 5.
3. Place the values from step 1 and 2 into their respective spot in equation 4-27.
4. Invert the 6-by-6 matrix and solve for the vector containing Δr and Δv .
5. Add these Δr and Δv values to the preliminary r and v -vectors.
6. Using these new r and v -vectors, calculate the new theoretical observation parameters at the six specified points in time the measurements were made

7. Compute the new residuals using the calculated data determined in step 6 with the observation data.
8. Repeat steps 2 through 7 until the residuals converge to a tolerable error.

Once these residuals converge, the new vectors can be transformed into TLEs as outlined in (Wertz, et al., 2001, p. 107) and (Bate, Mueller, & White, 1972, pp. 61-73), and can be used in orbit propagation and prediction software that uses one of the algorithms found in Chapter 3.

4.5 Conclusion

There are many different ways to determine the orbital elements of a spacecraft. By extracting one or more observation parameters by radar, camera, and spacecraft instruments, all information that can be gathered is useful for providing valuable data in determining and/or improving upon an orbit.

Table 4-1 briefly outlined the type of information different kinds of instruments can provide for orbit determination. The main observation data that ground-based RADAR locations can make usually consist of azimuth, elevation angles, and slant range data (Bate, Mueller, & White, 1972, p. 109), and thus more than one sighting is needed. If the RADAR location is capable of the aforementioned information and is outfitted to detect the rates of change in azimuth, elevation, and slant range, then only one sighting is needed and the orbit can be fully determined and a TLE can be generated.

On the other hand, using cameras require at least three sighting observations to determine the orbit of the satellite. These are the three sets of right ascensions and declinations of the satellite observation. However, these measurements are a lot harder to determine and thus another approach is generally taken. This approach uses the input parameters of Figure 4-3 to determine the right ascension and declination of each sighting observation.

Instantaneous measurements of this nature provide initial orbital estimates that include all secular and short-term periodic that are induced by the Earth and gravitational effects of other planets. Capturing all of these effects in equations for use in the force model is usually difficult. Thus, orbit propagation force models as outlined in Chapter 3 are generally used instead.

The force models explained in Chapter 3⁴² play an integral part in the differential correction process explained in section 4.4. Due to the inherent non-

⁴² Specifically, SGP4.

linear nature of gravitational and non-gravitational interactions, non-spherical mass distributions, and relativistic effects (no matter how small they might be) with a satellite, no single observation can fully determine the satellites orbital elements. Therefore, differential correction methods provide a way to correct for these disturbances and allow for a smoothed and averaged final set of TLEs per satellite.

Chapter 5 Conclusion

"There's nothing I believe in more strongly than getting young people interested in science and engineering, for a better tomorrow, for all humankind."

- Bill Nye

In the previous chapters, the building blocks have been laid out in how Keplerian elements are generated, disseminated, and propagated. In Chapter 2, the history of two-line elements and the type of information contained within were examined. Chapter 3 briefly described the history, development, and methodology of the two different kinds of techniques used for propagating the location of satellites. Lastly, Chapter 4 outlined how preliminary Keplerian elements are generated and further refined by using multiple observations in order to minimize positioning errors.

Even today, the smallest obtainable positioning error for LEO satellites is still relatively high (Table 5-1). As shown in Figure 4-4, the positioning error that a satellite experiences is still in the order of a couple hundred meters⁴³. Unfortunately, this error is only for the initial refined two-line element set. If the TLE is not regularly updated, the erroring effects of the simplified dynamics in the Simplified General Perturbation series propagators start to dominate, and over the course of a day, positioning uncertainties can grow at a rate of one to three

⁴³ This is about 350 meters RMS for the data shown in Figure 4-4.

kilometers a day (Vallado, Crawford, Hujsak, & Kelso, 2006) (Vallado & Agapov, 2010, p. 5).

Table 5-1. Common Errors in Different Stages of Orbit Determination. Note. RADAR errors were determined by using equation 8.8 in Curry's publication for a 1-degree beamwidth, S/R of 12, and k_m value of 1.6 (Curry, 2004, p. 170). Optical Source: Orbit Determination Results from Optical Measurements (Vallado & Agapov, 2010).

ERROR SOURCES	ERROR (RMS)		
	RADAR	Optical	Laser
Cross-Track	~ 400m	250 - 500m	N/A
Along-Track	~ 400m	500 - 7000m	N/A
Altitude	$\frac{c}{2B} \sim 10m^{44}$	400 - 1000m	5cm
TLE (after the Differential Correction process)	± 200 to 500 meters		
Each additional day without updating a TLE	an additional 1 to 3 kilometers ⁴⁵		

Furthermore, with over a thousand active satellites and over half-a-million cataloged space debris objects, space is - in all actuality - a very risky environment. Therefore, with large positioning errors, Earth-orbiting satellites have to either execute debris avoidance maneuvers, if capable, or risk collision. For that reason, it is imperative to have systems in place for generating two-line elements with the smallest errors possible and a system where the two-line elements are updated frequently. These two systems help provide the best possible positioning estimates of satellites while keeping positioning errors low.

As most satellites do not have a cross-track velocity component, the cross-track errors are *usually* the smallest (mainly for optical measurements) and remain the most stable (Vallado & Agapov, 2010, p. 7)⁴⁶. However, as a satellite is propagated forward in time, cross-track positioning uncertainties stem from two

⁴⁴ C - Speed of light; B - Signal bandwidth (Curry, Radar Measurement and Tracking, 2004, p. 166). Typical values are about 10 meters (Vetter, 2007, p. 241).
⁴⁵This depends on the altitude as lower altitudes result in higher errors due to higher drag effects (Vallado, Crawford, Hujsak, & Kelso, 2006, p. 33).
⁴⁶ Exclusive of laser ranging systems, as not all satellites are equipped with a reflector.

main sources: the inclination and right ascension of the ascending node of the satellite. Luckily, the inclination of the satellite remains relatively stable, but due to small fluctuations in the oblateness of the Earth, the right ascension of the ascending node drifts (Wertz, Collins, Dawson, Hönigsmann, & Potterveld, 1997, p. 270). This in turn causes a constant change in positioning uncertainty in the cross-track position component.

When it comes to along-track errors, there are two main sources: drag and time synchronization. Drag forces primarily dominate orbits below 800 kilometers (Wertz, Collins, Dawson, Hönigsmann, & Potterveld, 1997, p. 270). Thus, satellites constantly have to fight against this force. Time synchronization is just as important for ground-based orbit determination systems as well as satellite-based orbit determination systems due to the along-track direction experiencing very high velocities. Thus, any offset in clock times has the potential to cause large positioning errors in this direction.

Other sources of errors, along with their explanation concerning Orbit Determination systems, are found in *Mission Geometry; Orbit and Constellation Design and Management* (Wertz, et al., 2001, p. 270). An explanation of these individually is beyond the scope of this report, as most of them are already accounted for in the algorithms described in Chapter 3 and Chapter 4.

The purpose of this report was to gather, present, and direct the reader to the necessary information required in order to examine current ground- and satellite-based orbit determination systems. From this information, knowing accurately the position of the satellite is key to not only generating TLEs, but also in communicating with the satellite, creating more accurate measurements of what the satellite is observing, assessing the probability of satellite-satellite collisions, and if a collision occurs, determining where the collision happened.

Positioning errors from TLEs are still relatively large (Park, Park, Roh, & Choi, 2010) (Vallado & Agapov, 2010) (Vetter, 2007) and if not continually updated, increase every day. Computers no longer have the limitations imposed by the Honeywell 6080 mainframe computer from the 1980s. Therefore, it is about time that the performance of orbit propagators be reassessed in conjunction with ground- and satellite-measured data. Looking at this information, it can be determined if there exists some combination of data and an analytical orbit propagator that can provide better results than those currently used today while still being faster than a numerical-based model.

In order to keep these positing errors low, a method will be examined that looks at error propagation throughout the orbit propagators and uses the different analytical orbit propagators alongside measurements/properties of satellites. These results will be analyzed and compared to actual tracking data as well as numerical-based orbit propagation techniques. From this gathered data, a route that improves orbit determination via using instruments or positioning data can be assessed. These measurements/properties of satellites include, but are not limited to, durations of satellite eclipses, voltage data, received radio signal strengths, and Doppler shift waterfall graphs (Figure 5-2).

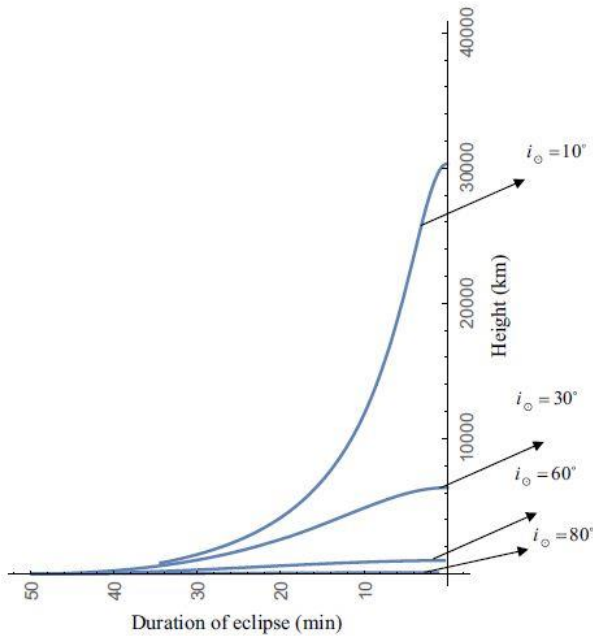


Figure 5-1. Eclipse Intervals vs. Altitude and Inclination. Adapted from "Eclipse Intervals for Satellites in Circular Orbit Under the Effects of Earth's Oblateness and Solar Radiation Pressure" by M. N. Ismail & et. al, 2015, *Journal of Astronomy and Geophysics*, 4,p. 120. Copyright 2015 by M. N. Ismail & et. al.

Since TLE-generated accuracies are known, how these accuracies can be improved should be examined. Thus, the questions that stem from this report become:

- Where are the highest sources of error during TLE generation? Can these errors be improved upon? If so, how?
- Are there any *direct* or *indirect* measurements/properties of satellites that can be used to further reduce the positioning error of the satellite? If so, where are these changes introduced?
- Is there a better orbit propagator that would yield better results under certain applications?
- Is there an on-board instrument that can aid in further reducing positioning errors? If not, could it be built and if so, what are the requirements that this instrument would need?

The duration of an eclipse is directly related to the altitude and angle between the satellite's orbital plane and the Sun, i_{\odot} , (Figure 5-1). Thus, by calculating the eclipse time using on-board measurements such as solar panel voltage data, the height of the satellite can be determined. Of course, the altitude of the satellite can be determined to about five centimeters using lasers and to about 10 meters using RADARs, but the question remains: Can this data prove to be of use along with differential correction to improve upon certain Keplerian elements of a satellite?

Radio properties also provide an interesting clue into the orbit of a satellite. By knowing the frequency that a satellite transmits on and the received frequency and strength as a function of time (Figure 5-2), it is possible to not only determine the range rate of the satellite, but also the distance⁴⁷, time of closest approach, and the time of acquisition and loss of signal⁴⁸. From this information, the actual pass duration of the satellite as well as the time of closest approach can be calculated. Furthermore, the range rate of the satellite can be calculated directly from the data presented in Figure 5-2. In addition, all of this data can be compared to the theoretical values. Thus, the orbital elements of the satellite can be refined so that both the measured and theoretical values match.

⁴⁷ Accounting for atmospheric attenuation.

⁴⁸ Assuming a clear horizon.

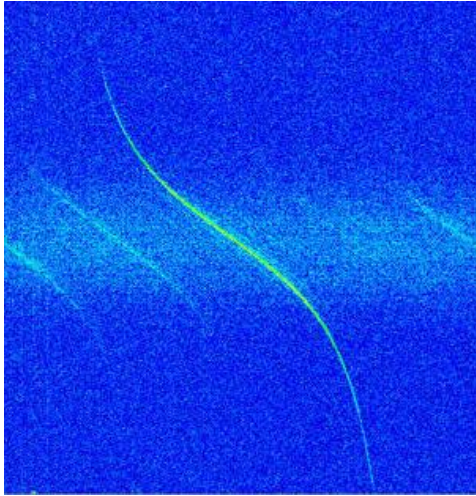


Figure 5-2. Waterfall Graph of a Satellite Pass. Note. The point in the middle of this line is the time of closest approach. The two outer points represent the acquisition and loss of signal of the satellite for this particular pass. Adapted from Sven's Space Place by Sven Grahn, 2007, Copyright 2007 by Sven Grahn.⁴⁹

Using *direct* or *indirect* data that already have large uncertainties could very well not improve Keplerian elements at all. In fact, it could make the Keplerian elements worse! Thus, an error analysis will need to be carried out throughout the whole orbit propagation and orbit determination problem to determine where these errors are and what kind of information can best contribute to lowering positioning errors of satellites than the current data sets used today. By closely examining orbit propagation models and the orbit determination problem, space for scientists, researchers, universities, and individuals to explore, conduct higher-quality research, and make new discoveries in a much safer environment will be made possible. How will this be done? The answer to this is what will be discovered.

⁴⁹ <http://www.svengrahn.pp.se/trackind/OdinSignal/OdinSignal.html>

Appendix A. LIST OF VARIABLES

Az	Azimuth [deg]
B	SGP8 drag coefficient [ER^{-1}]
B^*	SGP4 drag coefficient [ER^{-1}]
El	Elevation [deg]
GM	Gravitational Parameter
L	The Line-of-sight unit vector from ground station to satellite
M_o	Mean Anomaly [deg]
R	The geocentric position vector of a ground station
a	Semi-major axis [km]
e_o	Eccentricity [-]
f_G	Gravitational accelerations acting upon a satellite
f_{NG}	Non-gravitational accelerations acting upon a satellite
i_o	Inclination [deg]
n_o	Mean Motion [rev/day]
\dot{n}_o	The time rate of change of the mean motion [rev/day ²]
\ddot{n}_o	The time rate of change of \dot{n}_o [rev/day ³]
r	The geocentric position vector of a satellite
t	The time-of-flight between two points in space [sec]
Ω_o	Right Ascension of the Ascending Node [deg]
α	Right Ascension [deg]
δ	Declination [deg]
μ	Gravitational Parameter (GM) - Earth: 398600.4418 [km ³ /s ²]
Δv	The angle between two vectors [deg].
ρ_x	The tropospheric vector to the satellite in the x -direction
ω_o	Argument of Perigee [deg]

Appendix B. LIST OF ACRONYMS

AFGP	Air Force General Perturbation
CME	Coronal Mass Ejection
CPU	Central Processing Unit
DP4	Deep-Space Perturbation Theory Nr. 4
GPS	Global Positioning System
IGP	<i>Unknown</i>
IGRF	International Geomagnetic Reference Field
LEO	Low Earth Orbit (Altitude: from 160km to 2,000km)
MEO	Medium Earth Orbit (Altitude: from 2,000km to 35,786km)
NORAD	North American Aerospace Defense Command
RAAN	Right Ascension of the Ascending Node
RMS	Root Mean Square
SDP	Simplified Deep-Space Perturbation
SDP4	Simplified Deep-Space Perturbation Theory Nr. 4
SDP8	Simplified Deep-Space Perturbation Theory Nr. 8
SGP	Simplified General Perturbation
SGP4	Simplified General Perturbation Theory Nr. 4
SGP8	Simplified General Perturbation Theory Nr. 8
TLE	Two-Line Element
UTC	Coordinated Universal Time

Appendix C. TLE EXAMPLE

The following TLE was generated for the International Space Station on 8 October 2016 at 01:05:00 UTC. The first line is not a part of a TLE and only appears here to guide the reader in counting column numbers.

```
123456789 123456789 123456789 123456789 123456789 123456789 123456789
1 25544U 98067A 16280.54513569 .00016717 00000-0 10270-3 0 9035
2 25544 51.6411 222.5831 0007033 41.1186 319.0496 15.54057571 22306
```

Table C-1. A Complete Overview of a TLE.

COLUMN	CONTENT	EXAMPLE
LINE 1		
1	TLE Line Number	1
3-7	Satellite Number	25544
8	Satellite Classification	U - Unclassified
10-17	International Designator	98067A
19-32	Epoch Time	16280.54513569
34-43	$\dot{n}_0/2$	0.00016717
45-52	$\ddot{n}_0/6$	00000-0
54-61	B*	0.10270E-3
63	Ephemeris Type (Unused)	0
65-68	Element Set Number	903
69	Modulus 10 Checksum	5
LINE 2		
1	TLE Line Number	2
3-7	Satellite Number	25544
9-16	Inclination	51.6411 [deg]
18-25	RAAN	222.5831 [deg]
27-33	Eccentricity	0.0007033 [-]
35-42	Argument of Perigee	41.1186 [deg]
44-51	Mean Anomaly	319.0496 [deg]
53-63	Mean Motion	15.54057571 [Orbits/day]
64-68	Number of Orbits	2230
69	Modulus 10 Checksum	6

Bibliography

- AIG. (2016, October 31). *SGP-4 Propagator*. Retrieved from Astro Primer: SGP-4: <https://www.agi.com/resources/educational-alliance-program/astro-primer/primer106.htm>
- Bate, R. R., Mueller, D. D., & White, J. E. (1972). *Fundamentals of Astrodynamics*. New York, New York, United States of America: Dover Publications, Inc.
- Berget, R., Blake, J. B., Boden, D. G., Britton, W. R., Brodsky, R. F., Chomas, A., . . . Zimbelman, H. F. (1992). *Space Mission Analysis and Design* (2nd ed.). (J. R. Wertz, L. Markley, R. E. Münch, & J. F. Shea, Eds.) Torrance, California, United States of America: Microcosm, Inc.
- Bowen, J. A. (2009). *On-Board Orbit Determination and 3-Axis Attitude Determination for Picosatellite Applications*. San Luis Obispo, California: California Polytechnic State University.
- Brouwer, D. (1964). Solution of the Problem of Artificial Satellite Theory Without Drag. *The Astronomical Journal*, 378-396.
- Curry, G. R. (2004). *Radar Measurement and Tracking*. Artech House. Retrieved from http://www.artechhouse.com/uploads/public/documents/chapters/curry_816_ch08.pdf
- Curry, G. R. (2004). Radar Measurement and Tracking. In G. R. Curry, *Radar System Performance Modeling* (pp. 165-193). Artech House. Retrieved from http://www.artechhouse.com/uploads/public/documents/chapters/curry_816_ch08.pdf
- Herriges, D. L. (1988). *NORAD General Perturbation Theories: An Independent Analysis*. Cambridge, Massachusetts: Massachusetts Institute of Technology.
- Hoots, F. R., & Roehrich, R. L. (1980). *Models for Propagation of NORAD Element Sets*. Alexandria, Virginia: Defense Documentation Center.
- Hoots, F. R., & Roehrich, R. L. (1980). *Spacetrack Report No. 3: Models for Propagation of NORAD Element Sets*. Alexandria: Defense Documentation Center. Retrieved from <http://www.dtic.mil/dtic/tr/fulltext/u2/a093554.pdf>
- Ismail, M. N., Bakry, A., Selim, H. H., & Shehata, M. H. (2015). Eclipse Intervals for Satellites in Circular Orbit Under the Effects of Earth's

- Oblateness and Solar Radiation Pressure. *Journal of Astronomy and Geophysics*, 4(1), 117-122. doi:10.1016/2015.06.001
- Kelso, T. S. (2014, May 17). *Satellite Times: Computers & Satellites*. Retrieved from Celestrak: <https://celestrak.com/columns/>
- Kozai, Y. (1959). The Motion of a Close Earth Satellite. *The Astronomical Journal*, 367-377.
- Lane, M. H. (1965). The Development of an Artificial Satellite Theory Using a Power-Law Atmospheric Density Representation. *American Institute of Aeronautics and Astronautics*, 1-29.
- Lane, M. H., & Crawford, K. H. (1969). An Improved Analytical Drag Theory for the Artificial Satellite Problem. *American Institute of Aeronautics and Astronautics*, 1-11.
- Lane, M. H., & Hoots, F. R. (1979). *General Perturbations Theories Derived from the 1965 Lane Drag Theory*. Alexandria, Virginia: Defense Documentation Center.
- Leira, P. P., & Lara, M. (n.d.). An Implementation of SGP4 in Non-Singular Variables Using A Functional Paradigm.
- Magliacane, J. A. (2006, May). *PREDICT - A Satellite Tracking/Orbital Prediction Program*. Retrieved from <http://www.qsl.net/kd2bd/predict.html>
- Meeus, J. (2009). *Astronomical Algorithms* (2nd ed.). Richmond, Virginia, United States of America: Willmann-Bell, Inc.
- Miura, N. Z. (2009). *Comparison and Design of Simplified General Perturbation MODELS (SGP4) and Code for NASA Johnson Space Center, Orbital Debris Program Office*. San Luis Obispo, California: California Polytechnic State University.
- NIST. (n.d.). *Common View GPS Time Transfer*. Retrieved from National Institute of Standards and Technology: <http://tf.nist.gov/time/commonviewgps.htm>
- Ostrom, S. R. (1993). *Parallelization of the Air Force Space Command (AFSPACCOM) Satellite Motion Models*. Monterey, California: Naval Postgraduate School.
- Park, E.-S., Park, S.-Y., Roh, K.-M., & Choi, K.-H. (2010). Satellite Orbit Determination using a Batch Filter Based on the Unscented Transformation. *Aerospace Science and Technology*, 387-396.
- Psiaki, M. L. (1999, March-April). Autonomous Low-Earth-Orbit Determination from Magnetometer and Sun Sensor Data. *Journal of guidance, Control, and Dynamics*, 22(2), 296-304. doi:10.2514/2.4378

- Schattenberg, P. W. (2014). *BASICS-1: The Process of Converting Cartesian Coordinates into Keplerian Elements*. Delft, The Netherlands: Paul Schattenberg.
- Schattenberg, P. W. (2015). *Improvements in Ground Station Tracking Software*. Delft, The Netherlands: Paul Schattenberg.
- Staats, E. B. (1978, September 21). NORAD's Information Processing Improvement Program -- Will It Enhance Mission Capability? United States of America. Retrieved from <http://www.gao.gov/assets/130/123974.pdf>
- Vallado, D. A. (2007). *Fundamentals of Astrodynamics and Applications* (3rd ed.). Hawthorne, California, United States of America: Microcosm, Inc.
- Vallado, D. A., & Agapov, V. (2010). *Orbit Determination Results from Optical Measurements*. Madrid, Spain.
- Vallado, D. A., & McClain, W. D. (2004). *Fundamentals of Astrodynamics and Applications* (2nd ed., Vol. Space Technology Library). New York, New York: Microcosm Press.
- Vallado, D. A., Crawford, P., Hujsak, R., & Kelso, T. S. (2006). Revisiting Spacetrack Report #3. *American Institute of Aeronautics and Astronautics*.
- Vetter, J. R. (2007). Fifty Years of Orbit Determination: Development of Modern Astrodynamics Methods. *Johns Hopkins APL technical Digest*, 27(3), 239-252. Johns Hopkins Applied Physics Labs.
- Wertz, J. R., Collins, J. T., Dawson, S., Hönigsmann, H. J., & Potterveld, C. W. (1997). Autonomous Constellation Maintenance. In J. C. van der Ha (Ed.), *Mission Design & Implementation of Satellite Constellations* (pp. 263-274). Toulouse, France: Springer-Science+Business Media, B.V.
- Wertz, J. R., Meissinger, H. F., Newman, L. K., Smit, G. N., Bell, R. L., Collins, J. T., . . . Reynolds, H. (2001). *Mission Geometry; Orbit and Constellation Design and Management*. (J. R. Wertz, V. A. Chobotov, M. L. DeLorenzo, R. Doré, R. B. Giffen, G. Gurevich, . . . M. Sweeting, Eds.) El Segundo, California, United States of America: Microcosm, Inc.